



HAL
open science

C-mix: a high dimensional mixture model for censored durations, with applications to genetic data

Simon Bussy, Agathe Guilloux, Stéphane Gaïffas, Anne-Sophie Jannot

► To cite this version:

Simon Bussy, Agathe Guilloux, Stéphane Gaïffas, Anne-Sophie Jannot. C-mix: a high dimensional mixture model for censored durations, with applications to genetic data. *Statistical Methods in Medical Research*, 2019, 28 (5), pp.1523–1539. hal-01648389

HAL Id: hal-01648389

<https://hal.science/hal-01648389>

Submitted on 25 Nov 2017

HAL is a multi-disciplinary open access archive for the deposit and dissemination of scientific research documents, whether they are published or not. The documents may come from teaching and research institutions in France or abroad, or from public or private research centers.

L'archive ouverte pluridisciplinaire **HAL**, est destinée au dépôt et à la diffusion de documents scientifiques de niveau recherche, publiés ou non, émanant des établissements d'enseignement et de recherche français ou étrangers, des laboratoires publics ou privés.

C-mix: a high dimensional mixture model for censored durations, with applications to genetic data

Simon Bussy

Theoretical and Applied Statistics Laboratory
Pierre and Marie Curie University, Paris, France
email: simon.bussy@gmail.com

Agathe Guilloux

LaMME, UEVE and UMR 8071
Paris Saclay University, Evry, France
email: agathe.guilloux@math.cnrs.fr

Stéphane Gaïffas

CMAP Ecole polytechnique, Palaiseau, France
and LPMA, UMR CNRS 7599, Paris Diderot University, Paris, France
email: stephane.gaïffas@polytechnique.edu

Anne-Sophie Jannot

Biomedical Informatics and Public Health Department
European Georges Pompidou Hospital, Assistance Publique-Hôpitaux de Paris
and INSERM UMRS 1138, Centre de Recherche des Cordeliers, Paris, France
email: annesophie.jannot@aphp.fr

Abstract

We introduce a supervised learning mixture model for censored durations (C-mix) to simultaneously detect subgroups of patients with different prognosis and order them based on their risk. Our method is applicable in a high-dimensional setting, i.e. with a large number of biomedical covariates. Indeed, we penalize the negative log-likelihood by the Elastic-Net, which leads to a sparse parameterization of the model and automatically pinpoints the relevant covariates for the survival prediction. Inference is achieved using an efficient Quasi-Newton Expectation Maximization (QNEM) algorithm, for which we provide convergence properties. The statistical performance of the method is examined on an extensive Monte Carlo simulation study, and finally illustrated on three publicly available genetic cancer datasets with high-dimensional covariates. We show that our approach outperforms the state-of-the-art survival models in this context, namely both the CURE and Cox proportional hazards models penalized by the Elastic-Net, in terms of C-index, $AUC(t)$ and survival prediction. Thus, we propose a powerful tool for personalized medicine in cancerology.

Keywords. Coxs proportional hazards model; CURE model; Elastic-net regularization; High-dimensional estimation; Mixture duration model; Survival analysis

1 Introduction

Predicting subgroups of patients with different prognosis is a key challenge for personalized medicine, see for instance [Alizadeh et al. \[2000\]](#) and [Rosenwald et al. \[2002\]](#) where subgroups of patients with different survival rates are identified based on gene expression data. A substantial number of techniques can be found in the literature to predict the subgroup of a given patient in a classification setting, namely when subgroups are known in advance [[Golub et al., 1999](#), [Hastie et al., 2001](#), [Tibshirani et al., 2002](#)]. We consider in the present paper the much more difficult case where subgroups are unknown.

In this situation, a first widespread approach consists in first using unsupervised learning techniques applied on the covariates – for instance on the gene expression data [[Bhattacharjee et al., 2001](#), [Beer et al., 2002](#), [Sørlie et al., 2001](#)] – to define subsets of patients and then estimating the risks in each of them. The problem of such techniques is that there is no guarantee that the identified subgroups will have different risks. Another approach to subgroups identification is conversely based exclusively on the survival times: patients are then assigned to a low-risk or a high-risk group based on whether they were still alive [[Shipp et al., 2002](#), [Van't Veer et al., 2002](#)]. The problem here is that the resulting subgroups may not be biologically meaningful since the method do not use the covariates, and prognosis prediction based on covariates is not possible.

The method we propose uses both the survival information of the patients and its covariates in a supervised learning way. Moreover, it relies on the idea that exploiting the subgroups structure of the data, namely the fact that a portion of the population have a higher risk of early death, could improve the survival prediction of future patients (unseen during the learning phase).

We propose to consider a mixture of event times distributions in which the probabilities of belonging to each subgroups are driven by the covariates (e.g. gene expression data, patients characteristics, therapeutic strategy or omics covariates). Our C-mix model is hence part of the class of model-based clustering algorithms, as introduced in [Banfield and Raftery \[1993\]](#).

More precisely, to model the heterogeneity within the patient population, we introduce a latent variable $Z \in \{0, \dots, K - 1\}$ and our focus is on the conditional distribution of Z given the values of the covariates $X = x$. Now, conditionally on the latent variable Z , the distribution of duration time T is different, leading to a mixture in the event times distribution.

For a patient with covariates x , the conditional probabilities $\pi_k(x) = \mathbb{P}[Z = k|X = x]$ of belonging to the k -th risk group can be seen as scores, that can help decision-making for physicians. As a byproduct, it can also shed light on the effect of the covariates (which combination of biomedical markers are relevant to a given event of interest).

Our methodology differs from the standard survival analysis approaches in various ways, that we describe in this paragraph. First, the Cox proportional hazards (PH) model ([Cox \[1972\]](#)) (by far the most widely used in such a setting) is a regression model that describes the relation between intensity of events and covariates x

via

$$\lambda(t) = \lambda_0(t)\exp(x^\top \beta^{\text{cox}}), \quad (1)$$

where λ_0 is a baseline intensity, and β^{cox} is a vector quantifying the multiplicative impact on the hazard ratio of each covariate. As in our model, high-dimensional covariates can be handled, via e.g. penalization, see [Simon et al. \[2011\]](#). But it does not permit the stratification of the population in groups of homogeneous risks, hence does not deliver a simple tool for clinical practice. Moreover, we show in the numerical sections that the C-mix model can be trained very efficiently in high dimension, and outperforms the standard Cox PH model by far in the analysed datasets.

Other models consider mixtures of event times distributions. In the CURE model (see [Farewell \[1982\]](#) and [Kuk and Chen \[1992\]](#)), one fraction of the population is considered as cured (hence not subject to any risk). This can be very limiting, as for a large number of applications (e.g. rehospitalization for patients with chronic diseases or relapse for patients with metastatic cancer), all patients are at risk. We consider, in our model, that there is always an event risk, no matter how small. Other mixture models have been considered in survival analysis: see [Kuo and Peng \[2000\]](#) for a general study about mixture model for survival data or [De Angelis et al. \[1999\]](#) in a cancer survival analysis setting, to name but a few. Unlike our algorithm, none of these algorithms considers the high dimensional setting.

A precise description of the model is given in [Section 2](#). [Section 3](#) focuses on the regularized version of the model with an Elastic-Net penalization to exploit dimension reduction and prevent overfitting. Inference is presented under this framework, as well as the convergence properties of the developed algorithm. [Section 4](#) highlights the simulation procedure used to evaluate the performances and compares it with state-of-the-art models. In [Section 5](#), we apply our method to genetic datasets. Finally, we discuss the obtained results in [Section 6](#).

2 A censored mixture model

Let us present the survival analysis framework. We assume that, the conditional density of the duration T given $X = x$ is a mixture

$$f(t|X = x) = \sum_{k=0}^{K-1} \pi_k(x) f_k(t; \alpha_k)$$

of $K \geq 1$ densities f_k , for $t \geq 0$ and $\alpha_k \in \mathbb{R}^{d_k}$ some parameters to estimate. The weights combining these distributions depend on the patient biomedical covariates x and are such that

$$\sum_{k=0}^{K-1} \pi_k(x) = 1. \quad (2)$$

This is equivalent to saying that conditionally on a latent variable $Z = k \in \{0, \dots, K-1\}$, the density of T at time $t \geq 0$ is $f_k(t; \alpha_k)$, and we have

$$\mathbb{P}[Z = k|X = x] = \pi_k(x) = \pi_{\beta_k}(x)$$

where $\beta_k = (\beta_{k,1}, \dots, \beta_{k,d}) \in \mathbb{R}^d$ denotes a vector of coefficients that quantifies the impact of each biomedical covariates on the probability that a patient belongs to the k -th group. Consider a logistic link function for these weights given by

$$\pi_{\beta_k}(x) = \frac{e^{x^\top \beta_k}}{\sum_{k=0}^{K-1} e^{x^\top \beta_k}}. \quad (3)$$

The hidden status Z has therefore a multinomial distribution $\mathcal{M}(\pi_{\beta_0}(x), \dots, \pi_{\beta_{K-1}}(x))$. The intercept term is here omitted without loss of generality.

In practice, information loss occurs of right censoring type. This is taken into account in our model by introducing the following: a time $C \geq 0$ when the individual “leaves” the target cohort, a right-censored duration Y and a censoring indicator Δ , defined by

$$Y = \min(T, C) \quad \text{and} \quad \Delta = \mathbb{1}_{\{T \leq C\}},$$

where $\min(a, b)$ denotes the minimum between two numbers a and b , and $\mathbb{1}$ denotes the indicator function.

In order to write a likelihood and draw inference, we make the two following hypothesis.

Hypothesis 1 T and C are conditionally independent given Z and X .

Hypothesis 2 C is independent of Z .

Hypothesis 1 is classical in survival analysis [Klein and Moeschberger, 2005], while Hypothesis 2 is classical in survival mixture models [Kuo and Peng, 2000, De Angelis et al., 1999]. Under this hypothesis, denoting g the density of the censoring C , F the cumulative distribution function corresponding to a given density f , $\bar{F} = 1 - F$ and $F(y^-) = \lim_{\substack{u \rightarrow y \\ u \leq y}} F(u)$, we have

$$\begin{aligned} \mathbb{P}[Y \leq y, \Delta = 1] &= \mathbb{P}[T \leq y, T \leq C] = \int_0^y f(u) \bar{G}(u) du \quad \text{and} \\ \mathbb{P}[Y \leq y, \Delta = 0] &= \mathbb{P}[C \leq y, C < T] = \int_0^y g(u) \bar{F}(u) du. \end{aligned}$$

Then, denoting $\theta = (\alpha_0, \dots, \alpha_{K-1}, \beta_0, \dots, \beta_{K-1})^\top$ the parameters to infer and considering an independent and identically distributed (i.i.d.) cohort of n patients $(x_1, y_1, \delta_1), \dots, (x_n, y_n, \delta_n) \in \mathbb{R}^d \times \mathbb{R}_+ \times \{0, 1\}$, the log-likelihood of the C-mix model can be written

$$\begin{aligned} \ell_n(\theta) = \ell_n(\theta; \mathbf{y}, \boldsymbol{\delta}) &= n^{-1} \sum_{i=1}^n \left\{ \delta_i \log \left[\bar{G}(y_i^-) \sum_{k=0}^{K-1} \pi_{\beta_k}(x_i) f_k(y_i; \alpha_k) \right] \right. \\ &\quad \left. + (1 - \delta_i) \log \left[g(y_i) \sum_{k=0}^{K-1} \pi_{\beta_k}(x_i) \bar{F}_k(y_i^-; \alpha_k) \right] \right\}, \end{aligned}$$

where we use the notations $\mathbf{y} = (y_1, \dots, y_n)^\top$ and $\boldsymbol{\delta} = (\delta_1, \dots, \delta_n)^\top$. Note that from now on, all computations are done conditionally on the covariates $(x_i)_{i=1, \dots, n}$. An important fact is that we *do not need to know or parametrize* \bar{G} nor g , namely the distribution of the censoring, for inference in this model (since all \bar{G} and g terms vanish in Equation (6)).

3 Inference of C-mix

In this section, we describe the procedure for estimating the parameters of the C-mix model. We begin by presenting the Quasi-Newton Expectation Maximization (QNEM) algorithm we use for inference. We then focus our study on the convergence properties of the algorithm.

3.1 QNEM algorithm

In order to avoid overfitting and to improve the prediction power of our model, we use Elastic-Net regularization [Zou and Hastie, 2005] by minimizing the penalized objective

$$\ell_n^{\text{pen}}(\theta) = -\ell_n(\theta) + \sum_{k=0}^{K-1} \gamma_k \left((1 - \eta) \|\beta_k\|_1 + \frac{\eta}{2} \|\beta_k\|_2^2 \right), \quad (4)$$

where we add a linear combination of the lasso (ℓ_1) and ridge (squared ℓ_2) penalties for a fixed $\eta \in [0, 1]$, tuning parameter γ_k , and where we denote $\|\beta_k\|_p = \left(\sum_{i=1}^d |\beta_{k,i}|^p \right)^{1/p}$ the ℓ_p -norm of β_k . One advantage of this regularization method is its ability to perform model selection (the lasso part) and pinpoint the most important covariates relatively to the prediction objective. On the other hand, the ridge part allows to handle potential correlation between covariates [Zou and Hastie, 2005]. Note that in practice, the intercept is not regularized.

In order to derive an algorithm for this objective, we introduce a so-called Quasi-Newton Expectation Maximization (QNEM), being a combination between an EM algorithm [Dempster et al., 1977] and a L-BFGS-B algorithm [Zhu et al., 1997]. For the EM part, we need to compute the negative completed log-likelihood (here scaled by n^{-1}), namely the negative joint distribution of \mathbf{y} , $\boldsymbol{\delta}$ and $\mathbf{z} = (z_1, \dots, z_n)^\top$. It can be written

$$\begin{aligned} \ell_n^{\text{comp}}(\theta) &= \ell_n^{\text{comp}}(\theta; \mathbf{y}, \boldsymbol{\delta}, \mathbf{z}) \\ &= -n^{-1} \sum_{i=1}^n \left\{ \delta_i \left[\sum_{k=0}^{K-1} \mathbf{1}_{\{z_i=k\}} \left(\log \pi_{\beta_k}(x_i) + \log f_k(y_i; \alpha_k) \right) + \log \bar{G}(y_i^-) \right] \right. \\ &\quad \left. + (1 - \delta_i) \left[\sum_{k=0}^{K-1} \mathbf{1}_{\{z_i=k\}} \left(\log \pi_{\beta_k}(x_i) + \log \bar{F}_k(y_i^-; \alpha_k) \right) + \log g(y_i) \right] \right\}. \end{aligned} \quad (5)$$

Suppose that we are at step $l + 1$ of the algorithm, with current iterate denoted $\theta^{(l)} = (\alpha_0^{(l)}, \dots, \alpha_{K-1}^{(l)}, \beta_0^{(l)}, \dots, \beta_{K-1}^{(l)})^\top$. For the E-step, we need to compute the expected log-likelihood given by

$$Q_n(\theta, \theta^{(l)}) = \mathbb{E}_{\theta^{(l)}}[\ell_n^{\text{comp}}(\theta) | \mathbf{y}, \boldsymbol{\delta}].$$

We note that

$$q_{i,k}^{(l)} = \mathbb{E}_{\theta^{(l)}}[\mathbf{1}_{\{z_i=k\}} | y_i, \delta_i] = \mathbb{P}_{\theta^{(l)}}[z_i = k | y_i, \delta_i] = \frac{\Lambda_{k,i}^{(l)}}{\sum_{r=0}^{K-1} \Lambda_{r,i}^{(l)}} \quad (6)$$

with

$$\Lambda_{k,i}^{(l)} = [f_k(y_i; \alpha_k^{(l)}) \bar{G}(y_i^-)]^{\delta_i} [g(y_i) \bar{F}_k(y_i^-; \alpha_k^{(l)})]^{1-\delta_i} \pi_{\beta_k^{(l)}}(x_i) \quad (7)$$

so that $Q_n(\theta, \theta^{(l)})$ is obtained from (5) by replacing the two $\mathbb{1}_{\{z_i=k\}}$ occurrences with $q_{i,k}^{(l)}$. Depending on the chosen distributions f_k , the M-step can either be explicit for the updates of α_k (see Section 3.3 below for the geometric distributions case), or obtained using a minimization algorithm otherwise.

Let us focus now on the update of β_k in the M-step of the algorithm. By denoting

$$R_{n,k}^{(l)}(\beta_k) = -n^{-1} \sum_{i=1}^n q_{i,k}^{(l)} \log \pi_{\beta_k}(x_i)$$

the quantities involved in Q_n that depend on β_k , the update for β_k therefore requires to minimize

$$R_{n,k}^{(l)}(\beta_k) + \gamma_k \left((1 - \eta) \|\beta_k\|_1 + \frac{\eta}{2} \|\beta_k\|_2^2 \right). \quad (8)$$

The minimization Problem (8) is a convex problem. It looks like the logistic regression objective, where labels are not fixed but softly encoded by the expectation step (computation of $q_{i,k}^{(l)}$ above, see Equation (6)).

We minimize (8) using the well-known L-BFGS-B algorithm [Zhu et al., 1997]. This algorithm belongs to the class of quasi-Newton optimization routines, which solve the given minimization problem by computing approximations of the inverse Hessian matrix of the objective function. It can deal with differentiable convex objectives with box constraints. In order to use it with ℓ_1 penalization, which is not differentiable, we use the trick borrowed from Andrew and Gao [2007]: for $a \in \mathbb{R}$, write $|a| = a_+ + a_-$, where a_+ and a_- are respectively the positive and negative part of a , and add the constraints $a_+ \geq 0$ and $a_- \geq 0$. Namely, we rewrite the minimization problem (8) as the following differentiable problem with box constraints

$$\begin{aligned} \text{minimize} \quad & R_{n,k}^{(l)}(\beta_k^+ - \beta_k^-) + \gamma_k(1 - \eta) \sum_{j=1}^d (\beta_{k,j}^+ + \beta_{k,j}^-) + \gamma_k \frac{\eta}{2} \|\beta_k^+ - \beta_k^-\|_2^2 \\ \text{subject to} \quad & \beta_{k,j}^+ \geq 0 \text{ and } \beta_{k,j}^- \geq 0 \text{ for all } j \in \{1, \dots, d\}, \end{aligned} \quad (9)$$

where $\beta_k^\pm = (\beta_{k,1}^\pm, \dots, \beta_{k,d}^\pm)^\top$. The L-BFGS-B solver requires the exact value of the gradient, which is easily given by

$$\frac{\partial R_{n,k}^{(l)}(\beta_k)}{\partial \beta_k} = -n^{-1} \sum_{i=1}^n q_{i,k}^{(l)} (1 - \pi_{\beta_k}(x_i)) x_i. \quad (10)$$

In Algorithm 1, we describe the main steps of the QNEM algorithm to minimize the function given in Equation (4).

The penalization parameters γ_k are chosen using cross-validation, see Section A of Appendices for precise statements about this procedure and about other numerical details.

Algorithm 1: QNEM Algorithm for inference of the C-mix model

Require: Training data $(x_i, y_i, \delta_i)_{i \in \{1, \dots, n\}}$; starting parameters $(\alpha_k^{(0)}, \beta_k^{(0)})_{k \in \{0, \dots, K-1\}}$; tuning parameters $\gamma_k \geq 0$.

- 1: **for** $l = 0, \dots$, until convergence **do**
- 2: Compute $(q_{i,k}^{(l)})_{k \in \{0, \dots, K-1\}}$ using Equation (6).
- 3: Compute $(\alpha_k^{(l+1)})_{k \in \{0, \dots, K-1\}}$.
- 4: Compute $(\beta_k^{(l+1)})_{k \in \{0, \dots, K-1\}}$ by solving (9) with the L-BFGS-B algorithm.
- 5: **end for**
- 6: **return** Last parameters $(\alpha_k^{(l)}, \beta_k^{(l)})_{k \in \{0, \dots, K-1\}}$.

3.2 Convergence to a stationary point

We are addressing here convergence properties of the QNEM algorithm described in Section 3.1 for the minimization of the objective function defined in Equation (4). Let us denote

$$Q_n^{\text{pen}}(\theta, \theta^{(l)}) = Q_n(\theta, \theta^{(l)}) + \sum_{k=0}^{K-1} \gamma_k ((1 - \eta) \|\beta_k\|_1 + \frac{\eta}{2} \|\beta_k\|_2^2).$$

Convergence properties of the EM algorithm in a general setting are well known, see Wu [1983]. In the QNEM algorithm, since we only improve $Q_n^{\text{pen}}(\theta, \theta^{(l)})$ instead of a minimization of $Q_n(\theta, \theta^{(l)})$, we are not in the EM algorithm setting but in a so called generalized EM (GEM) algorithm setting [Dempster et al., 1977]. For such an algorithm, we do have the descent property, in the sense that the criterion function given in Equation (4) is reduced at each iteration, namely

$$\ell_n^{\text{pen}}(\theta^{(l+1)}) \leq \ell_n^{\text{pen}}(\theta^{(l)}).$$

Let us make two hypothesis.

Hypothesis 3 *The duration densities f_k are such that ℓ_n^{pen} is bounded for all θ .*

Hypothesis 4 *$Q_n^{\text{pen}}(\theta, \theta^{(l)})$ is continuous in θ and $\theta^{(l)}$, and for any fixed $\theta^{(l)}$, $Q_n^{\text{pen}}(\theta, \theta^{(l)})$ is a convex function in θ and is strictly convex in each coordinate of θ .*

Under Hypothesis 3, $l \mapsto \ell_n^{\text{pen}}(\theta^{(l)})$ decreases monotonically to some finite limit. By adding Hypothesis 4, convergence of the QNEM algorithm to a stationary point can be shown. In particular, the stationary point is here a local minimum.

Theorem 1 *Under Hypothesis 3 and 4, and considering the QNEM algorithm for the criterion function defined in Equation (4), every cluster point $\bar{\theta}$ of the sequence $\{\theta^{(l)}; l = 0, 1, 2, \dots\}$ generated by the QNEM algorithm is a stationary point of the criterion function defined in Equation (4).*

A proof is given in Section B of Appendices.

3.3 Parameterization

Let us discuss here the parametrization choices we made in the experimental part. First, in many applications - including the one addressed in Section 5 - we are interested in identifying one subgroup of the population with a high risk of adverse event compared to the others. Then, in the following, we consider $Z \in \{0, 1\}$ where $Z = 1$ means high-risk of early death and $Z = 0$ means low risk. Moreover, in such a setting where $K = 2$, one can compare the learned groups by the C-mix and the ones learned by the CURE model in terms of survival curves (see Figure 5).

To simplify notations and given the constraint formulated in Equation 2, we set $\beta_0 = 0$ and we denote $\beta = \beta_1$ and $\pi_\beta(x)$ the conditional probability that a patient belongs to the group with high risk of death, given its covariates x .

In practice, we deal with discrete times in days. It turns out that the times of the data used for applications in Section 5 is well fitted by Weibull distributions. This choice of distribution is very popular in survival analysis, see for instance Klein and Moeschberger [2005]. We then first derive the QNEM algorithm with

$$f_k(t; \alpha_k) = (1 - \phi_k)^{t^{\mu_k}} - (1 - \phi_k)^{(t+1)^{\mu_k}}$$

with here $\alpha_k = (\phi_k, \mu_k) \in (0, 1) \times \mathbb{R}_+$, ϕ_k being the scale parameter and μ_k the shape parameter of the distribution.

As explained in the following Section 4, we select the best model using a cross-validation procedure based on the C-index metric, and the performances are evaluated according to both C-index and $\text{AUC}(t)$ metrics (see Sections 4.3 for details). Those two metrics have the following property: if we apply any mapping on the marker vector (predicted on a test set) such that the order between all vector coefficient values is conserved, then both C-index and $\text{AUC}(t)$ estimates remain unchanged. In other words, by denoting $(M_i)_{i \in \{1, \dots, n_{\text{test}}\}}$ the vector of markers predicted on a test set of n_{test} individuals, if ψ is a function such that for all $(i, j) \in \{1, \dots, n_{\text{test}}\}^2$, $(M_i < M_j \Rightarrow \psi(M_i) < \psi(M_j))$, then both C-index and $\text{AUC}(t)$ estimates induced by $(M_i)_{i \in \{1, \dots, n_{\text{test}}\}}$ or by $(\psi(M_i))_{i \in \{1, \dots, n_{\text{test}}\}}$ are the same.

The order in the marker coefficients is actually paramount when the performances are evaluated according to the mentioned metrics. Furthermore, it turns out that empirically, if we add a constraint on the mixture of Weibull that enforces an *order like* relation between the two distributions f_0 and f_1 , the performances are improved. To be more precise, the constraint to impose is that the two density curves do not intersect. We then choose to impose the following: the two scale parameters are equal, *i.e.* $\phi_0 = \phi_1 = \phi$. Indeed under this hypothesis, we do have that for all $\phi \in (0, 1)$, $(\mu_0 < \mu_1 \Rightarrow \forall t \in \mathbb{R}_+, f_0(t; \alpha_0) > f_1(t; \alpha_1))$.

With this Weibull parameterization, updates for α_k are not explicit in the QNEM algorithm, and consequently require some iterations of a minimization algorithm. Seeking to have explicit updates for α_k , we then derive the algorithm with geometric distributions instead of Weibull (geometric being a particular case of Weibull with $\mu_k = 1$), namely $f_k(t; \alpha_k) = \alpha_k(1 - \alpha_k)^{t-1}$ with $\alpha_k \in (0, 1)$.

With this parameterization, we obtain from Equation (7)

$$\begin{aligned} \Lambda_{1,i}^{(l)} &= [\alpha_1^{(l)}(1 - \alpha_1^{(l)})^{y_i-1}]^{\delta_i} [(1 - \alpha_1^{(l)})^{y_i}]^{1-\delta_i} \pi_{\beta^{(l)}}(x_i) \quad \text{and} \\ \Lambda_{0,i}^{(l)} &= [\alpha_0^{(l)}(1 - \alpha_0^{(l)})^{y_i-1}]^{\delta_i} [(1 - \alpha_0^{(l)})^{y_i}]^{1-\delta_i} (1 - \pi_{\beta^{(l)}}(x_i)), \end{aligned}$$

which leads to the following explicit M-step

$$\alpha_0^{(l+1)} = \frac{\sum_{i=1}^n \delta_i (1 - q_i^{(l)})}{\sum_{i=1}^n (1 - q_i^{(l)}) y_i} \quad \text{and} \quad \alpha_1^{(l+1)} = \frac{\sum_{i=1}^n \delta_i q_i^{(l)}}{\sum_{i=1}^n q_i^{(l)} y_i}.$$

In this setting, implementation is hence straightforward. Note that Hypothesis 3 and 4 are immediately satisfied with this geometric parameterization.

In Section 5, we note that performances are similar for the C-mix model with Weibull or geometric distributions on all considered biomedical datasets. The geometric parameterization leading to more straightforward computations, it is the one used to parameterize the C-mix model in what follows, if not otherwise stated. Let us focus now on the performance evaluation of the C-mix model and its comparison with the Cox PH and CURE models, both regularized with the Elastic-Net.

4 Performance evaluation

In this section, we first briefly introduce the models we consider for performance comparisons. Then, we provide details regarding the simulation study and data generation. The chosen metrics for evaluating performances are then presented, followed by the results.

4.1 Competing models

The first model we consider is the Cox PH model penalized by the Elastic-Net, denoted Cox PH in the following. In this model introduced in Cox [1972], the partial log-likelihood is given by

$$\ell_n^{\text{cox}}(\beta) = n^{-1} \sum_{i=1}^n \delta_i (x_i^\top \beta - \log \sum_{i': y_{i'} \geq y_i} \exp(x_{i'}^\top \beta)).$$

We use respectively the R packages `survival` and `glmnet` [Simon et al., 2011] for the partial log-likelihood and the minimization of the following quantity

$$-\ell_n^{\text{cox}}(\beta) + \gamma((1 - \eta)\|\beta\|_1 + \frac{\eta}{2}\|\beta\|_2^2),$$

where γ is chosen by the same cross-validation procedure than the C-mix model, for a given η (see Section A of Appendices. Ties are handled via the Breslow approximation of the partial likelihood [Breslow, 1972]).

We remark that the model introduced in this paper cannot be reduced to a Cox model. Indeed, the C-mix model intensity can be written (in the geometric case)

$$\lambda(t) = \frac{\alpha_1(1 - \alpha_1)^{t-1} + \alpha_0(1 - \alpha_0)^{t-1} \exp(x^\top \beta)}{(1 - \alpha_1)^t + (1 - \alpha_0)^t \exp(x^\top \beta)},$$

while it is given by Equation (1) in the Cox model.

Finally, we consider the CURE Farewell [1982] model penalized by the Elastic-Net and denoted CURE in the following, with a logistic function for the incidence

part and a parametric survival model for $S(t|Z = 1)$, where $Z = 0$ means that patient is cured, $Z = 1$ means that patient is not cured, and $S(t) = \exp(-\int_0^t \lambda(s)ds)$ denotes the survival function. In this model, we then have $S(t|Z = 0)$ constant and equal to 1. We add an Elastic-Net regularization term, and since we were not able to find any open source package where CURE models were implemented with a regularized objective, we used the QNEM algorithm in the particular case of CURE model. We just add the constraint that the geometric distribution $\mathcal{G}(\alpha_0)$ corresponding to the cured group of patients ($Z = 0$) has a parameter $\alpha_0 = 0$, which does not change over the algorithm iterations. The QNEM algorithm can be used in this particular case, where some terms have disappeared from the completed log-likelihood, since in the CURE model case we have $\{i \in \{1, \dots, n\} : z_i = 0, \delta_i = 1\} = \emptyset$. Note that in the original introduction of the CURE model in [Farewell \[1982\]](#), the density of uncured patients directly depends on individual patient covariates, which is not the case here.

We also give additional simulation settings in Section C of Appendices. First, the case where $d \gg n$, including a comparison of the screening strategy we use in Section 5 with the iterative sure independence screening [\[Fan et al., 2010\]](#) (ISIS) method. We also add simulations where data is generated according to the C-mix model with gamma distributions instead of geometric ones, and include the accelerated failure time model [\[Wei, 1992\]](#) (AFT) in the performances comparison study.

4.2 Simulation design

In order to assess the proposed method, we perform an extensive Monte Carlo simulation study. Since we want to compare the performances of the 3 models mentioned above, we consider 3 simulation cases for the time distribution: one for each competing model. We first choose a coefficient vector $\beta = (\underbrace{\nu, \dots, \nu}_s, 0, \dots, 0) \in \mathbb{R}^d$, with $\nu \in \mathbb{R}$ being the value of the active coefficients and $s \in \{1, \dots, d\}$ a sparsity parameter. For a desired low-risk patients proportion $\pi_0 \in [0, 1]$, the high-risk patients index set is given by

$$\mathcal{H} = \{ \lfloor (1 - \pi_0) \times n \rfloor \text{ random samples without replacement} \} \subset \{1, \dots, n\},$$

where $\lfloor a \rfloor$ denotes the largest integer less than or equal to $a \in \mathbb{R}$. For the generation of the covariates matrix, we first take $[x_{ij}] \in \mathbb{R}^{n \times d} \sim \mathcal{N}(0, \Sigma(\rho))$, with $\Sigma(\rho)$ a $(d \times d)$ Toeplitz covariance matrix [\[Mukherjee and Maiti, 1988\]](#) with correlation $\rho \in (0, 1)$. We then add a $\text{gap} \in \mathbb{R}^+$ value for patients $i \in \mathcal{H}$ and subtract it for patients $i \notin \mathcal{H}$, only on active covariates plus a proportion $r_{cf} \in [0, 1]$ of the non-active covariates considered as confusion factors, that is

$$x_{ij} \leftarrow x_{ij} \pm \text{gap for } j \in \{1, \dots, s, \dots, \lfloor (d - s)r_{cf} \rfloor\}.$$

Note that this is equivalent to generate the covariates according to a gaussian mixture.

Then we generate $Z_i \sim \mathcal{B}(\pi_\beta(x_i))$ in the C-mix or CURE simulation case, where $\pi_\beta(x_i)$ is computed given Equation (3), with geometric distributions for

the durations (see Section 3.3). We obtain $T_i \sim \mathcal{G}(\alpha_{Z_i})$ in the C-mix case, and $T_i \sim \infty \mathbb{1}_{\{Z_i=0\}} + \mathcal{G}(\alpha_1) \mathbb{1}_{\{Z_i=1\}}$ in the CURE case. For the Cox PH model, we take $T_i \sim -\log(U_i) \exp(-x_i^\top \beta)$, with $U_i \sim \mathcal{U}([0, 1])$ and where $\mathcal{U}([a, b])$ stands for the uniform distribution on a segment $[a, b]$.

The distribution of the censoring variable C_i is geometric $\mathcal{G}(\alpha_c)$, with $\alpha_c \in (0, 1)$. The parameter α_c is tuned to maintain a desired censoring rate $r_c \in [0, 1]$, using a formula given in Section D of Appendices. The values of the chosen hyper parameters are summarized in Table 6.

Table 1: Hyper-parameters choice for simulation

η	n	d	s	r_{cf}	ν	ρ	π_0	gap	r_c	α_0	α_1
0.1	100, 200, 500	30, 100	10	0.3	1	0.5	0.75	0.1, 0.3, 1	0.2, 0.5	0.01	0.5

Note that when simulating under the CURE model, the proportion of censored time events is at least equal to π_0 : we then choose $\pi_0 = 0.2$ for the CURE simulations only.

Finally, we want to assess the stability of the C-mix model in terms of variable selection and compare it to the CURE and Cox PH models. To this end, we follow the same simulation procedure explained in the previous lines. For each simulation case, we make vary the two hyper-parameters that impact the most the stability of the variable selection, that is the gap varying in $[0, 2]$ and the confusion rate r_{cf} varying in $[0, 1]$. All other hyper-parameters are the same than in Table 6, except $s = 150$ and with the choice $(n, d) = (200, 300)$. For a given hyper-parameters configuration (gap, r_{cf}), we use the following approach to evaluate the variable selection power of the models. Denoting $\tilde{\beta}_i = |\hat{\beta}_i| / \max\{|\hat{\beta}_i|, i \in \{1, \dots, d\}\}$, if we consider that $\tilde{\beta}_i$ is the predicted probability that the true β_i equals ν , then we are in a binary prediction setting and we use the resulting AUC of this problem. Explicit examples of such AUC computations are given in Section E of Appendices.

4.3 Metrics

We detail in this section the metrics considered to evaluate risk prediction performances. Let us denote by M the marker under study. Note that $M = \pi_{\hat{\beta}}(X)$ in the C-mix and the CURE model cases, and $M = \exp(X^\top \hat{\beta}^{\text{cox}})$ in the Cox PH model case. We denote by h the probability density function of marker M , and assume that the marker is measured once at $t = 0$.

For any threshold ξ , cumulative true positive rates and dynamic false positive rates are two functions of time respectively defined as $\text{TPR}^{\text{C}}(\xi, t) = \mathbb{P}[M > \xi | T \leq t]$ and $\text{FPR}^{\text{D}}(\xi, t) = \mathbb{P}[M > \xi | T > t]$. Then, as introduced in Heagerty et al. [2000], the cumulative dynamic time-dependent AUC is defined as follows

$$\text{AUC}^{\text{C,D}}(t) = \int_{-\infty}^{\infty} \text{TPR}^{\text{C}}(\xi, t) \left| \frac{\partial \text{FPR}^{\text{D}}(\xi, t)}{\partial \xi} \right| d\xi,$$

that we simply denote $\text{AUC}(t)$ in the following. We use the Inverse Probability of Censoring Weighting (IPCW) estimate of this quantity with a Kaplan-Meier esti-

mator of the conditional survival function $\mathbb{P}[T > t|M = m]$, as proposed in [Blanche et al. \[2013\]](#) and already implemented in the R package `timeROC`.

A common concordance measure that does not depend on time is the C-index [[Harrell et al., 1996](#)] defined by

$$\mathcal{C} = \mathbb{P}[M_i > M_j | T_i < T_j],$$

with $i \neq j$ two independent patients (which does not depend on i, j under the i.i.d. sample hypothesis). In our case, T is subject to right censoring, so one would typically consider the modified \mathcal{C}_τ defined by

$$\mathcal{C}_\tau = \mathbb{P}[M_i > M_j | Y_i < Y_j, Y_i < \tau],$$

with τ corresponding to the fixed and prespecified follow-up period duration [[Heagerty and Zheng, 2005](#)]. A Kaplan-Meier estimator for the censoring distribution leads to a nonparametric and consistent estimator of \mathcal{C}_τ [[Uno et al., 2011](#)], already implemented in the R package `survival`.

Hence in the following, we consider both $\text{AUC}(t)$ and C-index metrics to assess performances.

4.4 Results of simulation

We present now the simulation results concerning the C-index metric in the case $(d, r_c) = (30, 0.5)$ in [Table 2](#). See [Section F](#) of [Appendices](#) for results on other configurations for (d, r_c) . Each value is obtained by computing the C-index average and standard deviation (in parenthesis) over 100 simulations. The $\text{AUC}(t)$ average (bold line) and standard deviation (bands) over the same 100 simulations are then given in [Figure 1](#), where $n = 100$. Note that the value of the gap can be viewed as a difficulty level of the problem, since the higher the value of the gap, the clearer the separation between the two populations (low risk and high risk patients).

The results measured both by $\text{AUC}(t)$ and C-index lead to the same conclusion: the C-mix model almost always leads to the best results, even under model misspecification, *i.e.* when data is generated according to the CURE or Cox PH model. Namely, under CURE simulations, C-mix and CURE give very close results, with a strong improvement over Cox PH. Under Cox PH and C-mix simulations, C-mix outperforms both Cox PH and CURE. Surprisingly enough, this exhibits a strong generalization property of the C-mix model, over both Cox PH and CURE. Note that this phenomenon is particularly strong for small gap values, while with an increasing gap (or an increasing sample size n), all procedures barely exhibit the same performance. It can be first explained by the non parametric baseline function in the Cox PH model, and second by the fact that unlike the Cox PH model, the C-mix and CURE models exploit directly the mixture aspect.

Finally, [Figure 2](#) gives the results concerning the stability of the variable selection aspect of the competing models. The C-mix model appears to be the best method as well considering the variable selection aspect, even under model misspecification. We notice a general behaviour of our method that we describe in the following, which is also shared by the CURE model only when the data is simulated according to itself, and which justifies the log scale for the gap to clearly distinguish the three

following phases. For very small gap values (less than 0.2), the confusion rate r_{cf} does not impact the variable selection performances, since adding very small gap values to the covariates is almost imperceptible. This means that the resulting AUC is the same when there is no confusion factors and when $r_{cf} = 1$ (that is when there are half active covariates and half confusion ones). For medium gap values (saying between 0.2 and 1), the confusion factors are more difficult to identify by the model as their number goes up (that is when r_{cf} increases), which is precisely the confusion factors effect we expect to observe. Then, for large gap values (more than 1), the model succeeds in vanishing properly all confusion factors since the two subpopulations are more clearly separated regarding the covariates, and the problem becomes naturally easier as the gap increases.

5 Application to genetic data

In this section, we apply our method on three genetic datasets and compare its performance to the Cox PH and CURE models. We extracted normalized expression data and survival times Y in days from breast invasive carcinoma (BRCA, $n = 1211$), glioblastoma multiforme (GBM, $n = 168$) and kidney renal clear cell carcinoma (KIRC, $n = 605$).

These datasets are available on The Cancer Genome Atlas (TCGA) platform, which aims at accelerating the understanding of the molecular basis of cancer through the application of genomic technologies, including large-scale genome sequencing. For each patient, 20531 covariates corresponding to the normalized gene expressions are available. We randomly split all datasets into a training set and a test set (30% for testing, cross-validation is done on the training).

We compare the three models both in terms of C-index and $AUC(t)$ on the test sets. Inference of the Cox PH model fails in very high dimension on the considered data with the `glmnet` package. We therefore make a first variable selection (screening) among the 20531 covariates. To do so, we compute the C-index obtained by univariate Cox PH models (not to confer advantage to our method), namely Cox PH models fitted on each covariate separately. We then ordered the obtained 20531 C-indexes by decreasing order and extracted the top $d = 100$, $d = 300$ and $d = 1000$ covariates. We then apply the three methods on the obtained covariates.

The results in terms of $AUC(t)$ curves are given in Figure 3 for $d = 300$, where we distinguish the C-mix model with geometric or Weibull distributions.

Then it appears that the performances are very close in terms of $AUC(t)$ between the C-mix model with geometric or Weibull distributions, which is also validated if we compare the corresponding C-index for these two parameterizations in Table 3.

Similar conclusions in terms of C-index, $AUC(t)$ and computing time can be made on all considered datasets and for any choice of d . Hence, as already mentioned in Section 3.3, we only concentrate on the geometric parameterization for the C-mix model. The results in terms of C-index are then given in Table 4.

A more direct approach to compare performances between models, rather than only focus on the marker order aspect, is to predict the survival of patients in the test set within a specified short time. For the Cox PH model, the survival

Table 2: Average C-index on 100 simulated data and standard deviation in parenthesis, with $d = 30$ and $r_c = 0.5$. For each configuration, the best result appears in bold.

Simulation	gap	Estimation								
		$n = 100$			$n = 200$			$n = 500$		
		C-mix	CURE	Cox PH	C-mix	CURE	Cox PH	C-mix	CURE	Cox PH
C-mix	0.1	0.786 (0.057)	0.745 (0.076)	0.701 (0.075)	0.792 (0.040)	0.770 (0.048)	0.739 (0.055)	0.806 (0.021)	0.798 (0.023)	0.790 (0.024)
	0.3	0.796 (0.055)	0.739 (0.094)	0.714 (0.088)	0.794 (0.036)	0.760 (0.058)	0.744 (0.055)	0.801 (0.021)	0.784 (0.027)	0.783 (0.026)
	1	0.768 (0.062)	0.734 (0.084)	0.756 (0.066)	0.766 (0.043)	0.736 (0.054)	0.764 (0.042)	0.772 (0.026)	0.761 (0.027)	0.772 (0.025)
CURE	0.1	0.770 (0.064)	0.772 (0.062)	0.722 (0.073)	0.790 (0.038)	0.790 (0.038)	0.758 (0.049)	0.798 (0.025)	0.799 (0.024)	0.787 (0.025)
	0.3	0.733 (0.073)	0.732 (0.072)	0.686 (0.072)	0.740 (0.053)	0.741 (0.053)	0.714 (0.060)	0.751 (0.029)	0.751 (0.029)	0.738 (0.030)
	1	0.659 (0.078)	0.658 (0.078)	0.635 (0.070)	0.658 (0.053)	0.658 (0.053)	0.647 (0.047)	0.657 (0.031)	0.657 (0.031)	0.656 (0.032)
Cox PH	0.1	0.940 (0.041)	0.937 (0.044)	0.850 (0.097)	0.959 (0.021)	0.958 (0.020)	0.915 (0.042)	0.964 (0.012)	0.964 (0.012)	0.950 (0.016)
	0.3	0.956 (0.030)	0.955 (0.029)	0.864 (0.090)	0.966 (0.020)	0.965 (0.020)	0.926 (0.043)	0.968 (0.013)	0.969 (0.012)	0.959 (0.016)
	1	0.983 (0.016)	0.985 (0.015)	0.981 (0.019)	0.984 (0.012)	0.985 (0.011)	0.988 (0.010)	0.984 (0.007)	0.985 (0.006)	0.990 (0.005)

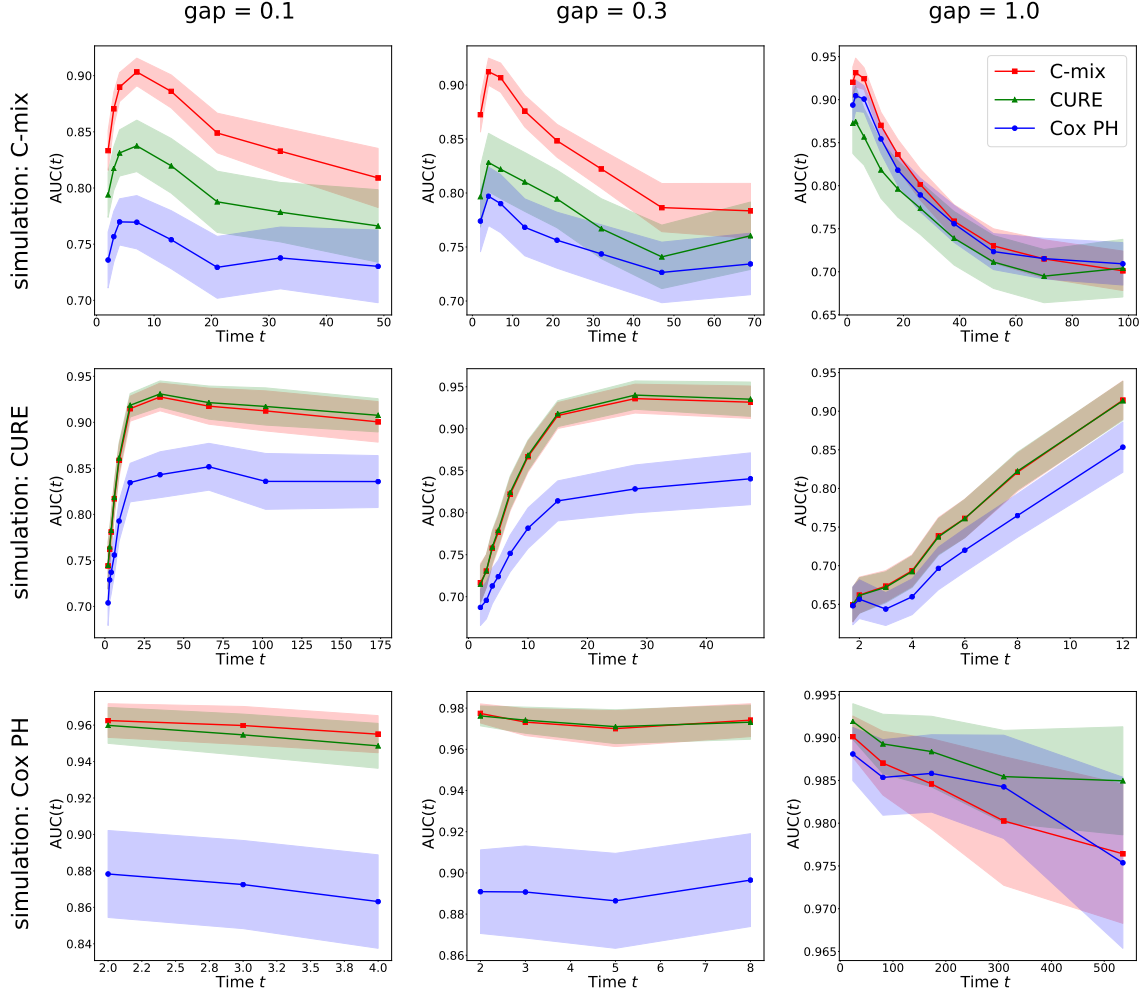


Figure 1: Average (bold lines) and standard deviation (bands) for $AUC(t)$ on 100 simulated data with $n = 100$, $d = 30$ and $r_c = 0.5$. Rows correspond to the model simulated (cf. Section 4.2) while columns correspond to different gap values (the problem becomes more difficult as the gap value decreases). Surprisingly, our method gives almost always the best results, even under model misspecification (see Cox PH and CURE simulation cases on the second and third rows).

Table 3: C-index comparison between geometric or Weibull parameterizations for the C-mix model on the three TCGA data sets considered (with $d = 300$). In all cases, results are very similar for the two distribution choices.

Parameterization		Geometric	Weibull
Cancer	BRCA	0.782	0.780
	GBM	0.755	0.754
	KIRC	0.849	0.835

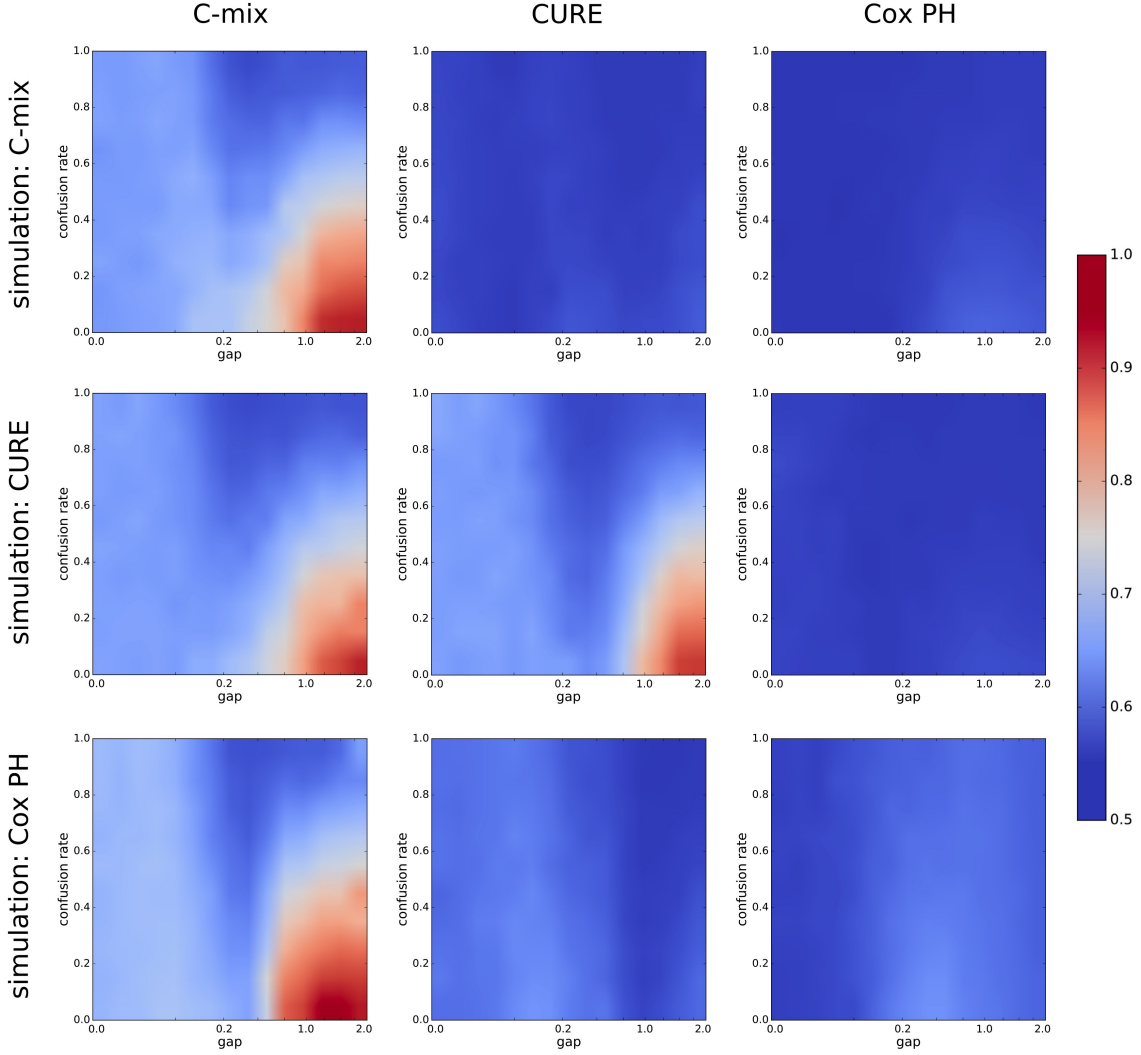


Figure 2: Average AUC calculated according to Section 4.2 and obtained after 100 simulated data for each (gap, r_{cf}) configuration (a grid of 20x20 different configurations is considered). A gaussian interpolation is then performed to obtain smooth figures. Note that the gap values are \log -scaled. Rows correspond to the model simulated while columns correspond to the model under consideration for the variable selection evaluation procedure. Our method gives the best results in terms of variable selection, even under model misspecification.

$\mathbb{P}[T_i > t | X_i = x_i]$ for patient i in the test set is estimated by

$$\hat{S}_i(t | X_i = x_i) = [\hat{S}_0^{\text{cox}}(t)]^{\exp(x_i^\top \hat{\beta}^{\text{cox}})},$$

where \hat{S}_0^{cox} is the estimated survival function of baseline population ($x = 0$) obtained using the Breslow estimate of λ_0 [Breslow, 1972]. For the CURE or the C-mix models, it is naturally estimated by

$$\hat{S}_i(t | X_i = x_i) = \pi_{\hat{\beta}}(x_i) \hat{S}_1(t) + (1 - \pi_{\hat{\beta}}(x_i)) \hat{S}_0(t),$$

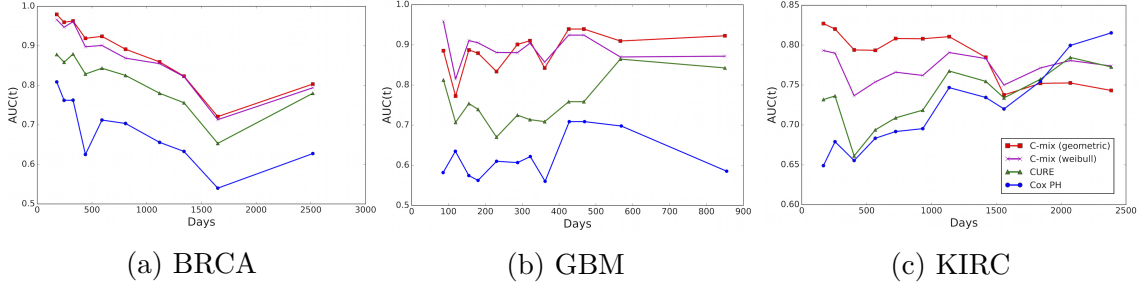


Figure 3: AUC(t) comparison on the three TCGA data sets considered, for $d = 300$. We observe that C-mix model leads to the best results (higher is better) and outperforms both Cox PH and CURE in all cases. Results are similar in terms of performances for the C-mix model with geometric or Weibull distributions.

Table 4: C-index comparison on the three TCGA data sets considered. In all cases, C-mix gives the best results (in bold).

Cancer	Model	BRCA			GBM			KIRC		
		C-mix	CURE	Cox PH	C-mix	CURE	Cox PH	C-mix	CURE	Cox PH
d	100	0.792	0.764	0.705	0.826	0.695	0.571	0.768	0.732	0.716
	300	0.782	0.753	0.723	0.849	0.697	0.571	0.755	0.691	0.698
	1000	0.817	0.613	0.577	0.775	0.699	0.592	0.743	0.690	0.685

where \hat{S}_0 and \hat{S}_1 are the Kaplan-Meier estimators [Kaplan and Meier, 1958] of the low and high risk subgroups respectively, learned by the C-mix or CURE models (patients with $\pi_{\hat{\beta}}(x_i) > 0.5$ are clustered in the high risk subgroup, others in the low risk one). The corresponding estimated survival curves are given in Figure 4. We observe that the subgroups obtained by the C-mix are more clearly separated in terms of survival than those obtained by the CURE model.

For a given time ϵ , one can now use $\hat{S}_i(\epsilon|X_i = x_i)$ for each model to predict whether or not $T_i > \epsilon$ on the test set, resulting on a binary classification problem that we assess using the classical AUC score. By moving ϵ within the first years of follow-up, since it is the more interesting for physicians in practice, one obtains the curves given in Figure 5.

Let us now focus on the runtime comparison between the models in Table 5. We choose the BRCA dataset to illustrate this point, since it is the larger one ($n = 1211$) and consequently provides more clearer time-consuming differences.

We also notice that despite using the same QNEM algorithm steps, our CURE model implementation is slower since convergence takes more time to be reached, as shows Figure 6.

In Section G of Appendices, the top 20 selected genes for each cancer type and for all models are presented (for $d = 300$). Literature on those genes is mined to estimate two simple scores that provide information about how related they are to cancer in general first, and second to cancer plus the survival aspect, according to scientific publications. It turns out that some genes have been widely studied in the literature (e.g. FLT3 for the GBM cancer), while for others, very few publications were retrieved (e.g. TRMT2B still for the GBM cancer).

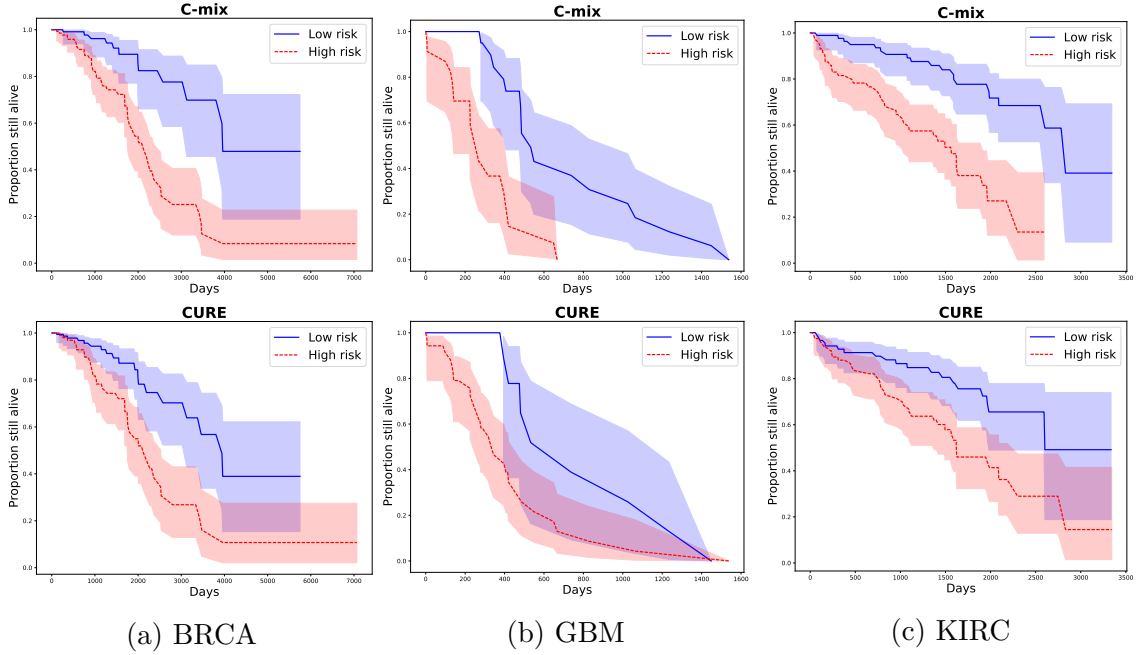


Figure 4: Estimated survival curves per subgroups (blue for low risk and red for high risk) with the corresponding 95 % confidence bands for the C-mix and CURE models: BRCA in column (a), GBM in column (b) and KIRC in column (c).

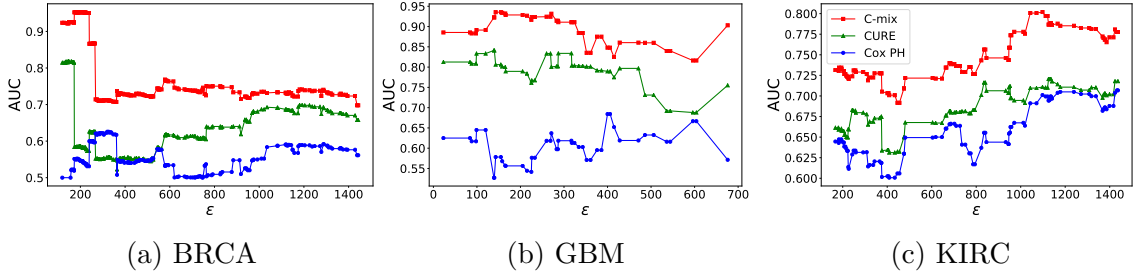


Figure 5: Comparison of the survival prediction performances between models on the three TCGA data sets considered (still with $d = 300$). Performances are, once again, much better for the C-mix over the two other standard methods.

Table 5: Computing time comparison in second on the BRCA dataset ($n = 1211$), with corresponding C-index in parenthesis and best result in bold in each case. This times concern the learning task for each model with the best hyper parameter selected after the cross validation procedure. It turns out that our method is by far the fastest in addition to providing the best performances. In particular, the QNEM algorithm is faster than the R implementation `glmnet`.

Model		C-mix	CURE	Cox PH
d	100	0.025 (0.792)	1.992 (0.764)	0.446 (0.705)
	300	0.027 (0.782)	2.343 (0.753)	0.810 (0.723)
	1000	0.139 (0.817)	12.067 (0.613)	2.145 (0.577)

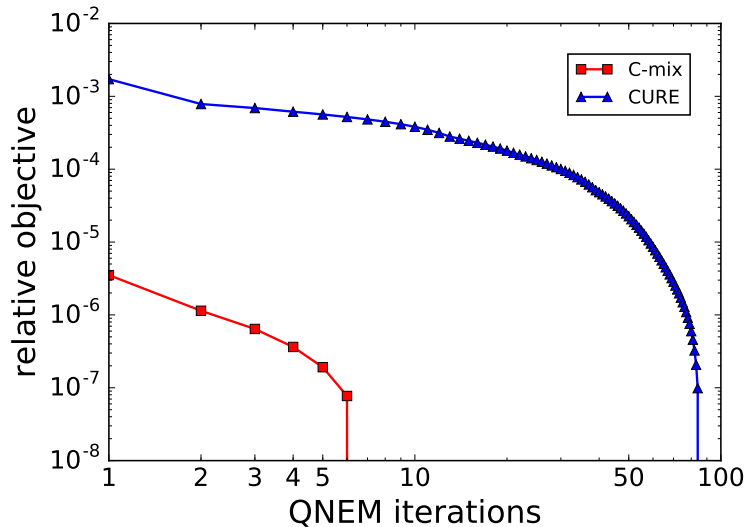


Figure 6: Convergence comparison between C-mix and CURE models through the QNEM algorithm. The relative objective is here defined at iteration l as $(\ell_n^{\text{pen}}(\theta^{(l)}) - \ell_n^{\text{pen}}(\hat{\theta})) / \ell_n^{\text{pen}}(\hat{\theta})$, where $\hat{\theta}$ is naturally the parameter vector returned at the end of the QNEM algorithm, that is once convergence is reached. Note that both iteration and relative objective axis are *log*-scaled for clarity. We observe that convergence for the C-mix model is dramatically faster than the CURE one.

6 Concluding remarks

In this paper, a mixture model for censored durations (C-mix) has been introduced, and a new efficient estimation algorithm (QNEM) has been derived, that considers a penalization of the likelihood in order to perform covariate selection and to prevent overfitting. A strong improvement is provided over the CURE and Cox PH approaches (both penalized by the Elastic-Net), which are, by far, the most widely used for biomedical data analysis. But more importantly, our method detects relevant subgroups of patients regarding their risk in a supervised learning procedure, and takes advantage of this identification to improve survival prediction over more standard methods. An extensive Monte Carlo simulation study has been carried out to evaluate the performance of the developed estimation procedure. It showed that our approach is robust to model misspecification. The proposed methodology has then been applied on three high dimensional datasets. On these datasets, C-mix outperforms both Cox PH and CURE, in terms of $\text{AUC}(t)$, C-index or survival prediction. Moreover, many gene expressions pinpointed by the feature selection aspect of our regularized method are relevant for medical interpretations (e.g. NFKBIA, LEF1, SUSD3 or FAIM3 for the BRCA cancer, see Zhou et al. [2007] or Oskarsson et al. [2011]), whilst others must involve further investigations in the genetic research community. Finally, our analysis provides, as a by-product, a new robust implementation of CURE models in high dimension.

Software

All the methodology discussed in this paper is implemented in Python. The code is available from <https://github.com/SimonBussy/C-mix> in the form of annotated programs, together with a notebook tutorial.

Acknowledgements

The results shown in this paper are based upon data generated by the TCGA Research Network and freely available from <http://cancergenome.nih.gov/>. *Conflict of Interest:* None declared.

Appendices

A Numerical details

Let us first give some details about the starting point of Algorithm 1. For all $k \in \{0, \dots, K-1\}$, we simply use $\beta_k^{(0)}$ as the zero vector, and for $\alpha_k^{(0)}$ we fit a censored parametric mixture model on $(y_i)_{i=1, \dots, n}$ with an EM algorithm.

Concerning the V-fold cross validation procedure for tuning γ_k , we use $V = 5$ and the cross-validation metric is the C-index. Let us precise that we choose γ_k as the largest value such that error is within one standard error of the minimum, and that a grid-search is made during the cross-validation on an interval $[\gamma_k^{\max} \times 10^{-4}, \gamma_k^{\max}]$, with γ_k^{\max} the interval upper bound computed in the following.

Let us consider the following convex minimization problem resulting from Equation (8), at a given step l :

$$\hat{\beta}_k \in \operatorname{argmin}_{\beta \in \mathbb{R}^d} R_{n,k}^{(l)}(\beta) + \gamma_k \left((1 - \eta) \|\beta\|_1 + \frac{\eta}{2} \|\beta\|_2^2 \right).$$

Regarding the grid of candidate values for γ_k , we consider $\gamma_k^1 \leq \gamma_k^2 \leq \dots \leq \gamma_k^{\max}$. At γ_k^{\max} , all coefficients $\hat{\beta}_{k,j}$ for $j \in \{1, \dots, d\}$ are exactly zero. The KKT conditions [Boyd and Vandenberghe, 2004] claim that

$$\begin{cases} \frac{\partial R_{n,k}^{(l)}(\hat{\beta}_k)}{\partial \beta_j} = \gamma_k (1 - \eta) \operatorname{sgn}(\hat{\beta}_{k,j}) + \eta \hat{\beta}_{k,j} & \forall j \in \hat{\mathcal{A}}_k \\ \left| \frac{\partial R_{n,k}^{(l)}(\hat{\beta}_k)}{\partial \beta_j} \right| < \gamma_k (1 - \eta) & \forall j \notin \hat{\mathcal{A}}_k \end{cases},$$

where $\hat{\mathcal{A}}_k = \{j \in \{1, \dots, d\} : \hat{\beta}_{k,j} \neq 0\}$ is the active set of the $\hat{\beta}_k$ estimator, and for all $x \in \mathbb{R} \setminus \{0\}$, $\operatorname{sgn}(x) = \mathbf{1}_{\{x>0\}} - \mathbf{1}_{\{x<0\}}$. Then, using (10), one obtains

$$\forall j \in \{1, \dots, d\}, \hat{\beta}_{k,j} = 0 \Rightarrow \forall j \in \{1, \dots, d\}, \left| n^{-1} \sum_{i=1}^n q_{i,k}^{(l)} \frac{1}{2} x_{ij} \right| < \gamma_k (1 - \eta)$$

Hence, we choose the following upper bound for the grid search interval during the cross-validation procedure

$$\gamma_k^{\max} = \frac{1}{2n(1-\eta)} \max_{j \in \{1, \dots, d\}} \sum_{i=1}^n |x_{ij}|.$$

B Proof of Theorem 1

Let us denote $D = \sum_{k=0}^{K-1} d_k + Kd$ the number of coordinates of θ so that one can write

$$\theta = (\theta_1, \dots, \theta_D) = (\alpha_0, \dots, \alpha_{K-1}, \beta_0, \dots, \beta_{K-1})^\top \in \Theta \subset \mathbb{R}^D.$$

We denote $\bar{\theta}$ a cluster point of the sequence $S = \{\theta^{(l)}; l = 0, 1, 2, \dots\}$ generated by the QNEM algorithm, *i.e.* $\forall \varepsilon > 0, V_\varepsilon(\bar{\theta}) \cap S \setminus \{\bar{\theta}\} \neq \emptyset$, with $V_\varepsilon(\bar{\theta})$ the epsilon-neighbourhood of $\bar{\theta}$. We want to prove that $\bar{\theta}$ is a stationary point of the non-differentiable function $\theta \mapsto \ell_n^{\text{pen}}(\theta)$, which means [Tseng, 2001]:

$$\forall r \in \mathbb{R}^D, \nu_n^{\text{pen} \prime}(\bar{\theta}; r) = \lim_{\zeta \rightarrow 0} \frac{\ell_n^{\text{pen}}(\bar{\theta} + r\zeta) - \ell_n^{\text{pen}}(\bar{\theta})}{\zeta} \geq 0. \quad (11)$$

The proof is inspired by Bertsekas [1995]. The conditional density of the complete data given the observed data can be written

$$k(\theta) = \frac{\exp(\ell_n^{\text{comp}}(\theta))}{\exp(\ell_n(\theta))}.$$

Then, one has

$$\ell_n^{\text{pen}}(\theta) = Q_n^{\text{pen}}(\theta, \theta^{(l)}) - H(\theta, \theta^{(l)}), \quad (12)$$

where we introduced $H(\theta, \theta^{(l)}) = \mathbb{E}_{\theta^{(l)}}[\log(k(\theta))]$. The key argument relies on the following facts that hold under Hypothesis (3) and (4):

- $Q_n^{\text{pen}}(\theta, \theta^{(l)})$ is continuous in θ and $\theta^{(l)}$,
- for any fixed $\theta^{(l)}$ (at the $(l+1)$ -th M step of the algorithm), $Q_n^{\text{pen}}(\theta, \theta^{(l)})$ is convex in θ and strictly convex in each coordinate of θ .

Let $r \in \mathbb{R}^D$ be an arbitrary direction, then Equations (11) and (12) yield

$$\ell_n^{\text{pen} \prime}(\bar{\theta}; r) = Q_{n, \bar{\theta}}^{\text{pen} \prime}(\bar{\theta}; r) - \langle \nabla H_{\bar{\theta}}(\bar{\theta}), r \rangle.$$

Hence, by Jensen's inequality we get

$$\forall \theta \in \Theta, H(\theta^{(l)}, \theta^{(l)}) \leq H(\theta, \theta^{(l)}), \quad (13)$$

and so $\theta \mapsto H_{\bar{\theta}}(\theta)$ is minimized for $\theta = \theta^{(l)}$, then we have $\nabla H_{\bar{\theta}}(\bar{\theta}) = 0$. It remains to prove that $Q_{n, \bar{\theta}}^{\text{pen} \prime}(\bar{\theta}; r) \geq 0$. Let us focus on the proof of the following expression

$$\forall x_1, Q_{n, \bar{\theta}}^{\text{pen}}(\bar{\theta}) \leq Q_{n, \bar{\theta}}^{\text{pen}}(x_1, \bar{\theta}_2, \dots, \bar{\theta}_D). \quad (14)$$

Denoting $w_i^{(l)} = (\theta_1^{(l+1)}, \dots, \theta_i^{(l+1)}, \theta_{i+1}^{(l)}, \dots, \theta_D^{(l)})$ and from the definition of the QNEM algorithm, we first have

$$Q_{n,\theta^{(l)}}^{\text{pen}}(\theta^{(l)}) \geq Q_{n,\theta^{(l)}}^{\text{pen}}(w_1^{(l)}) \geq \dots \geq Q_{n,\theta^{(l)}}^{\text{pen}}(w_{D-1}^{(l)}) \geq Q_{n,\theta^{(l)}}^{\text{pen}}(\theta^{(l+1)}), \quad (15)$$

and second for all x_1 , $Q_{n,\theta^{(l)}}^{\text{pen}}(w_1^{(l)}) \leq Q_{n,\theta^{(l)}}^{\text{pen}}(x_1, \theta_2^{(l)}, \dots, \theta_D^{(l)})$. Consequently, if $(w_1^{(l)})_{l \in \mathbb{N}}$ converges to $\bar{\theta}$, one obtains (14) by continuity taking the limit $l \rightarrow \infty$. Let us now suppose that $(w_1^{(l)})_{l \in \mathbb{N}}$ does not converge to $\bar{\theta}$, so that $(w_1^{(l)} - \theta^{(l)})_{l \in \mathbb{N}}$ does not converge to 0. Or equivalently: there exists a subsequence $(w_1^{(l_j)} - \theta^{(l_j)})_{j \in \mathbb{N}}$ not converging to 0.

Then, denoting $\psi^{(l_j)} = \|w_1^{(l_j)} - \theta^{(l_j)}\|_2$, we may assume that there exists $\bar{\psi} > 0$ such that $\forall j \in \mathbb{N}$, $\psi^{(l_j)} > \bar{\psi}$ by removing from the subsequence $(w_1^{(l_j)} - \theta^{(l_j)})_{j \in \mathbb{N}}$ any terms for which $\psi^{(l_j)} = 0$. Let $s_1^{(l_j)} = \frac{w_1^{(l_j)} - \theta^{(l_j)}}{\psi^{(l_j)}}$, so that $(s_1^{(l_j)})_{j \in \mathbb{N}}$ belongs to a compact set ($\|s_1^{(l_j)}\| = 1$) and then converges to $\bar{s}_1 \neq 0$. Let us fix some $\epsilon \in [0, 1]$, then $0 \leq \epsilon \bar{\psi} \leq \psi^{(l_j)}$. Moreover, $\theta^{(l_j)} + \epsilon \bar{\psi} s_1^{(l_j)}$ lies on the segment joining $\theta^{(l_j)}$ and $w_1^{(l_j)}$, and consequently belongs to Θ since Θ is convex. As $Q_{n,\theta^{(l_j)}}^{\text{pen}}(\cdot)$ is convex and $w_1^{(l_j)}$ minimizes this function over all values that differ from $\theta^{(l_j)}$ along the first coordinate, one has

$$\begin{aligned} Q_{n,\theta^{(l_j)}}^{\text{pen}}(w_1^{(l_j)}) &= Q_{n,\theta^{(l_j)}}^{\text{pen}}(\theta^{(l_j)} + \psi^{(l_j)} s_1^{(l_j)}) \\ &\leq Q_{n,\theta^{(l_j)}}^{\text{pen}}(\theta^{(l_j)} + \epsilon \bar{\psi} s_1^{(l_j)}) \\ &\leq Q_{n,\theta^{(l_j)}}^{\text{pen}}(\theta^{(l_j)}). \end{aligned} \quad (16)$$

We finally obtain

$$\begin{aligned} 0 &\leq Q_{n,\theta^{(l_j)}}^{\text{pen}}(\theta^{(l_j)}) - Q_{n,\theta^{(l_j)}}^{\text{pen}}(\theta^{(l_j)} + \epsilon \bar{\psi} s_1^{(l_j)}) \\ &\stackrel{(16)}{\leq} Q_{n,\theta^{(l_j)}}^{\text{pen}}(\theta^{(l_j)}) - Q_{n,\theta^{(l_j)}}^{\text{pen}}(w_1^{(l_j)}) \\ &\stackrel{(15)}{\leq} Q_{n,\theta^{(l_j)}}^{\text{pen}}(\theta^{(l_j)}) - Q_{n,\theta^{(l_j)}}^{\text{pen}}(\theta^{(l_j+1)}) \\ &\stackrel{(12)}{\leq} \ell_n^{\text{pen}}(\theta^{(l_j)}) - \ell_n^{\text{pen}}(\theta^{(l_j+1)}) + \underbrace{H_{\theta^{(l_j)}}(\theta^{(l_j)}) - H_{\theta^{(l_j)}}(\theta^{(l_j+1)})}_{\stackrel{(13)}{\leq} 0} \\ &\leq \ell_n^{\text{pen}}(\theta^{(l_j)}) - \ell_n^{\text{pen}}(\theta^{(l_j+1)}) \xrightarrow{j \rightarrow \infty} \ell_n^{\text{pen}}(\bar{\theta}) - \ell_n^{\text{pen}}(\bar{\theta}) = 0 \end{aligned}$$

By continuity of the function $Q_n^{\text{pen}}(x, y)$ in both x and y and taking the limit $j \rightarrow \infty$, we conclude that $\forall \epsilon \in [0, 1]$, $Q_{n,\bar{\theta}}^{\text{pen}}(\bar{\theta} + \epsilon \bar{\psi} \bar{s}_1) = Q_{n,\bar{\theta}}^{\text{pen}}(\bar{\theta})$. Since $\bar{\psi} \bar{s}_1 \neq 0$, this contradicts the strict convexity of $x_1 \mapsto Q_{n,\theta^{(l)}}^{\text{pen}}(x_1, \theta_2^{(l)}, \dots, \theta_D^{(l)})$ and establishes that $(w_1^{(l)})_{l \in \mathbb{N}}$ converges to $\bar{\theta}$.

Hence (14) is proved. Repeating the argument to each coordinate, we deduce that $\bar{\theta}$ is a coordinate-wise minimum, and finally conclude that $\ell_n^{\text{pen}'}(\bar{\theta}; r) \geq 0$ [Tseng, 2001]. Thus, $\bar{\theta}$ is a stationary point of the criterion function defined in Equation (4). □

C Additional comparisons

In this section, we consider two extra simulation settings. First, we consider the case $d \gg n$, which is the setting of our application on TCGA datasets. Then, we add another simulation case under the C-mix model using gamma distributions instead of geometric ones. The shared parameters in the two cases are given in Table 6.

Table 6: Hyper-parameters choice for simulation.

η	n	s	r_{cf}	ν	ρ	π_0	gap	r_c
0.1	250	50	0.5	1	0.5	0.75	0.1	0.5

C.1 Case $d \gg n$

Data is here generated under the C-mix model with $(\alpha_0, \alpha_1) = (0.1, 0.5)$ and $d \in \{200, 500, 1000\}$. The 3 models are trained on a training set and risk prediction is made on a test set. We also compare the 3 models when a dimension reduction step is performed at first, using two different screening methods. The first is based on univariate Cox PH models, namely the one we used in Section 5 of the paper (in our application to genetic data), where we select here the top 100 variables. This screening method is hence referred as “top 100” in the following. The second is the iterative sure independence screening (ISIS) method introduced in Fan et al. [2010], using the R package SIS Saldana and Feng [2016]. Prediction performances are compared in terms of C-index, while variable selection performances are compared in terms of AUC using the method detailed in Section E, and we also add two more classical scores [Fan et al., 2010] for comparison: the median ℓ_1 and squared ℓ_2 estimation errors, given by $\|\beta - \hat{\beta}\|_1$ and $\|\beta - \hat{\beta}\|_2$ respectively. Results are given in Table 7.

The C-mix model obtains constantly the best C-index performances in prediction, for all settings. Moreover, the “top 100” screening method improve the 3 models prediction power, while ISIS method only improve the Cox PH model prediction power. As expected, ISIS method significantly improve the Cox PH model in terms of variable selection and obtains the best results for $d = 500$ and 1000. Conclusions in terms of variable selection are the same relatively to the AUC, ℓ_1 and squared ℓ_2 estimation errors. Then, in the paper, we only focus on the AUC method detailed in Section E. Note that the Cox PH model obtains the best results in terms of variable selection with the two screening method, since both screening methods are based on the Cox PH model. Thus, one could improve the C-mix variable selection performances by simply use the “top 100” screening method with univariate C-mix, which was not the purpose of the section. Finally, the results obtained justify the screening strategy we use in Section 5 of the paper.

C.2 Case of times simulated with a mixture of gammas

We consider here the case where data is simulated under the C-mix model with gamma distributions instead of geometric ones, not to confer to the C-mix prior

Table 7: Average performances and standard deviation (in parenthesis) on 100 simulated data for different dimension d and different screening method (including no screening). For each configuration, the best result appears in bold.

d	screening	model	C-index	AUC	$\ \beta - \hat{\beta}\ _1$	$\ \beta - \hat{\beta}\ _2$
200	none	C-mix	0.716 (0.062)	0.653 (0.053)	51.540 (0.976)	7.254 (0.129)
		CURE	0.701 (0.067)	0.625 (0.052)	51.615 (1.275)	7.274 (0.122)
		Cox PH	0.672 (0.089)	0.608 (0.063)	199.321 (0.490)	99.679 (0.229)
	top 100	C-mix	0.737 (0.057)	0.682 (0.060)	52.297 (1.351)	7.381 (0.161)
		CURE	0.714 (0.060)	0.651 (0.050)	52.366 (1.382)	7.386 (0.134)
		Cox PH	0.692 (0.089)	0.630 (0.070)	52.747 (0.530)	7.946 (0.093)
	ISIS	C-mix	0.691 (0.049)	0.570 (0.011)	55.493 (1.624)	8.083 (0.394)
		CURE	0.685 (0.050)	0.571 (0.009)	54.461 (1.112)	7.848 (0.211)
		Cox PH	0.690 (0.049)	0.573 (0.011)	48.186 (0.366)	6.840 (0.037)
500	none	C-mix	0.710 (0.058)	0.642 (0.057)	51.627 (0.994)	7.277 (0.106)
		CURE	0.675 (0.057)	0.610 (0.052)	51.920 (2.411)	7.252 (0.138)
		Cox PH	0.624 (0.097)	0.567 (0.057)	499.610 (0.396)	157.997 (0.117)
	top 100	C-mix	0.735 (0.050)	0.694 (0.057)	53.161 (1.708)	7.433 (0.152)
		CURE	0.703 (0.054)	0.649 (0.042)	53.419 (1.818)	7.387 (0.133)
		Cox PH	0.682 (0.087)	0.633 (0.074)	49.465 (0.428)	6.937 (0.094)
	ISIS	C-mix	0.677 (0.051)	0.559 (0.013)	55.229 (1.831)	7.974 (0.375)
		CURE	0.671 (0.051)	0.559 (0.015)	54.187 (1.244)	7.754 (0.227)
		Cox PH	0.675 (0.051)	0.560 (0.016)	48.574 (0.614)	6.870 (0.054)
1000	none	C-mix	0.694 (0.063)	0.633 (0.066)	51.976 (1.921)	7.272 (0.141)
		CURE	0.657 (0.067)	0.598 (0.057)	52.078 (2.414)	7.236 (0.138)
		Cox PH	0.579 (0.092)	0.541 (0.050)	999.768 (0.316)	223.558 (0.067)
	top 100	C-mix	0.726 (0.050)	0.693 (0.040)	53.813 (1.592)	7.149 (0.115)
		CURE	0.685 (0.061)	0.653 (0.037)	54.146 (1.596)	7.383 (0.090)
		Cox PH	0.688 (0.076)	0.668 (0.064)	52.838 (0.558)	6.909 (0.077)
	ISIS	C-mix	0.653 (0.062)	0.553 (0.017)	53.760 (1.949)	7.269 (0.395)
		CURE	0.652 (0.061)	0.554 (0.015)	53.928 (1.288)	7.687 (0.236)
		Cox PH	0.652 (0.063)	0.553 (0.015)	51.826 (0.606)	6.895 (0.054)

information on the underlying survival distributions. Hence, one has

$$f_k(t; \iota_k, \zeta_k) = \frac{t^{\iota_k-1} e^{-\frac{t}{\zeta_k}}}{\zeta_k^{\iota_k} \Gamma(\iota_k)},$$

with ι_k the shape parameter, ζ_k the scale parameter and Γ the gamma function. For the simulations, we choose $(\iota_0, \zeta_0) = (5, 3)$ and $(\iota_1, \zeta_1) = (1.5, 1)$, so that density and survival curves are comparable with those in Section C.1, as illustrates Figure 7 below.

We also add another class of model for comparison in this context: the accelerated failure time model [Wei, 1992] (AFT); which can be viewed as a parametric Cox model. Indeed, the semi-parametric property of the Cox PH model could lower its performances compared to completely parametric models such as C-mix and CURE ones, especially in simulations where n is relatively small. We use the R package `AdapEnetClass` that implements AFT in a high dimensional setting us-

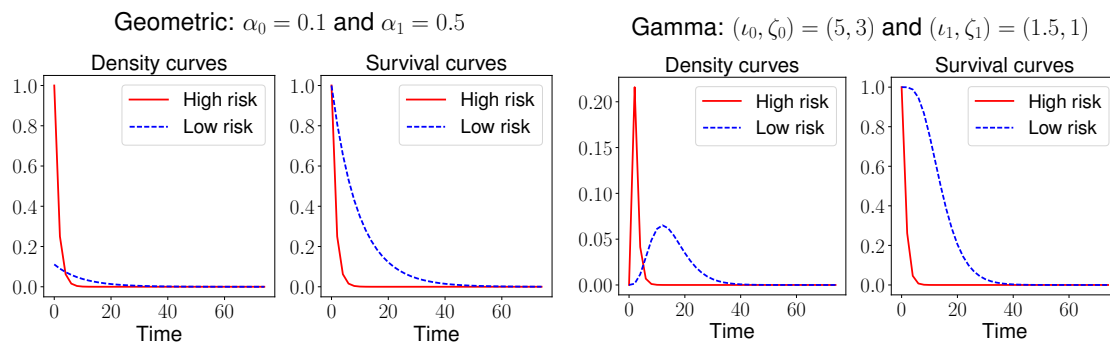


Figure 7: Comparison of the density and survival curves of geometrics laws used in Section C.1 and those used in this section. The supports are then relatively close.

ing two Elastic-Net regularization approaches [Khan and Shaw, 2016]: the adaptive Elastic-Net (denoted AEnet in the following) and the weighted Elastic-Net (denoted WEnet in the following). Results are given in Table 8 using the same metrics that in Section C.1.

Table 8: Average performances and standard deviation (in parenthesis) on 100 simulated data for different dimension d with the times simulated with a mixture of gammas. For each configuration, the best result appears in bold.

d	model	C-index	AUC	$\ \beta - \hat{\beta}\ _1$	$\ \beta - \hat{\beta}\ _2$
200	C-mix	0.701 (0.090)	0.659 (0.083)	51.339 (2.497)	7.186 (0.281)
	CURE	0.682 (0.058)	0.609 (0.037)	51.563 (1.071)	7.263 (0.097)
	Cox PH	0.664 (0.085)	0.605 (0.065)	199.337 (0.493)	99.686 (0.231)
	AEnet	0.631 (0.062)	0.577 (0.046)	54.651 (2.328)	7.713 (0.426)
	WEnet	0.620 (0.061)	0.544 (0.030)	58.861 (4.298)	8.568 (0.851)
500	C-mix	0.704 (0.100)	0.651 (0.084)	52.416 (2.311)	7.357 (0.231)
	CURE	0.687 (0.057)	0.609 (0.038)	52.041 (1.667)	7.262 (0.096)
	Cox PH	0.621 (0.101)	0.559 (0.057)	499.677 (0.381)	158.017 (0.113)
	AEnet	0.604 (0.061)	0.557 (0.030)	55.126 (1.693)	7.616 (0.316)
	WEnet	0.594 (0.065)	0.535 (0.021)	59.736 (2.777)	8.438 (0.626)
1000	C-mix	0.684 (0.097)	0.638 (0.088)	52.557 (3.746)	7.331 (0.277)
	CURE	0.658 (0.057)	0.603 (0.044)	53.120 (3.853)	7.273 (0.165)
	Cox PH	0.580 (0.092)	0.538 (0.053)	999.785 (0.334)	223.561 (0.071)
	AEnet	0.586 (0.058)	0.541 (0.024)	54.597 (1.312)	7.495 (0.299)
	WEnet	0.583 (0.054)	0.525 (0.017)	58.746 (2.260)	8.150 (0.551)

Hence, the C-mix model still gets the best results, both in terms of risk prediction and variable selection. Note that AFT with AEnet and WEnet outperforms the Cox model regularized by the Elastic-Net when $d = 1000$, but is still far behind the C-mix performances.

D Tuning of the censoring level

Suppose that we want to generate data following the procedure detailed in Section 4.2, in the C-mix with geometric distributions or CURE case. The question here is to choose α_c for a desired censoring rate r_c , and for some fixed parameters α_0 , α_1 and π_0 . We write

$$\begin{aligned} 1 - r_c = \mathbb{E}[\delta] &= \sum_{k=0}^{+\infty} \sum_{j=1}^{+\infty} [\alpha_0(1 - \alpha_0)^{j-1}\pi_0 + \alpha_1(1 - \alpha_1)^{j-1}(1 - \pi_0)] \alpha_c(1 - \alpha_c)^{j+k-1} \\ &= \frac{\alpha_0\pi_0[1 - (1 - \alpha_1)(1 - \alpha_c)] + \alpha_1(1 - \pi_0)[1 - (1 - \alpha_0)(1 - \alpha_c)]}{[1 - (1 - \alpha_0)(1 - \alpha_c)][1 - (1 - \alpha_1)(1 - \alpha_c)]}. \end{aligned}$$

Then, if we denote $\bar{r}_c = 1 - r_c$, $\bar{\alpha}_c = 1 - \alpha_c$, $\bar{\alpha}_0 = 1 - \alpha_0$, $\bar{\alpha}_1 = 1 - \alpha_1$ and $\bar{\pi}_0 = 1 - \pi_0$, we can choose α_c for a fixed r_c by solving the following quadratic equation

$$(\bar{r}_c \bar{\alpha}_0 \bar{\alpha}_1) \bar{\alpha}_c^2 + (\alpha_0 \pi_0 \bar{\alpha}_1 + \alpha_1 \bar{\pi}_0 \bar{\alpha}_0 - \bar{r}_c (\bar{\alpha}_1 + \bar{\alpha}_0)) \bar{\alpha}_c + (r_c - \alpha_0 \pi_0 - \alpha_1 \bar{\pi}_0) = 0,$$

for which one can prove that there is always a unique root in $(0, 1)$.

E Details on variable selection evaluation

Let us recall that the true underlying β used in the simulations is given by

$$\beta = \underbrace{(\nu, \dots, \nu)}_s, 0, \dots, 0 \in \mathbb{R}^d,$$

with s the sparsity parameter, being the number of “active” variables. To illustrate how we assess the variable selection ability of the considered models, we give in Figure 8 an example of β with $d = 100$, $\nu = 1$ and $s = 30$. We simulate data according to this vector (and to the C-mix model) with two different (gap, r_{cf}) values: $(0.2, 0.7)$ and $(1, 0.3)$. Then, we give the two corresponding estimated vectors $\hat{\beta}$ learned by the C-mix on this data.

Denoting $\tilde{\beta}_i = |\hat{\beta}_i| / \max\{|\hat{\beta}_i|, i \in \{1, \dots, d\}\}$, we consider that $\tilde{\beta}_i$ is the predicted probability that the true coefficient β_i corresponding to i -th covariate equals ν . Then, we are in a binary prediction setting where each $\tilde{\beta}_i$ predicts $\beta_i = \nu$ for all $i \in \{1, \dots, d\}$. We use the resulting AUC to assess the variable selection obtained through $\hat{\beta}$.

F Extended simulation results

Table 9 bellow presents the results of simulation for the configurations $(d, r_c) = (30, 0.2)$, $(100, 0.2)$ and $(100, 0.5)$.

Table 9: Average C-index and standard deviation (in parenthesis) on 100 simulated data for different configurations (d, r_c) , with geometric distributions for the C-mix model. For each configuration, the best result appears in bold.

		Estimation									
		$n = 100$		$n = 200$		$n = 500$					
Simulation	gap	C-mix	CURE	Cox PH	C-mix	CURE	Cox PH	C-mix	CURE	Cox PH	
		$(d, r_c) = (30, 0.2)$									
C-mix	0.1	0.753 (0.055)	0.637 (0.069)	0.658 (0.081)	0.762 (0.034)	0.664 (0.070)	0.704 (0.051)	0.767 (0.023)	0.686 (0.062)	0.749 (0.025)	
	0.3	0.756 (0.050)	0.599 (0.073)	0.657 (0.075)	0.761 (0.033)	0.600 (0.064)	0.713 (0.050)	0.757 (0.020)	0.565 (0.049)	0.740 (0.021)	
	1	0.723 (0.059)	0.710 (0.063)	0.714 (0.062)	0.723 (0.042)	0.718 (0.044)	0.721 (0.040)	0.727 (0.026)	0.723 (0.028)	0.726 (0.025)	
Cox PH	0.1	0.918 (0.042)	0.872 (0.070)	0.850 (0.081)	0.938 (0.022)	0.911 (0.032)	0.906 (0.034)	0.949 (0.014)	0.940 (0.018)	0.938 (0.017)	
	0.3	0.935 (0.034)	0.906 (0.051)	0.877 (0.066)	0.947 (0.019)	0.932 (0.028)	0.915 (0.030)	0.952 (0.013)	0.950 (0.015)	0.949 (0.015)	
	1	0.956 (0.031)	0.958 (0.032)	0.919 (0.065)	0.960 (0.018)	0.969 (0.016)	0.951 (0.024)	0.958 (0.011)	0.968 (0.011)	0.967 (0.010)	
		$(d, r_c) = (100, 0.2)$									
		Estimation									
		$n = 100$		$n = 200$		$n = 500$					
Simulation	gap	C-mix	CURE	Cox PH	C-mix	CURE	Cox PH	C-mix	CURE	Cox PH	
C-mix	0.1	0.736 (0.048)	0.601 (0.081)	0.656 (0.066)	0.757 (0.037)	0.629 (0.079)	0.697 (0.057)	0.767 (0.020)	0.659 (0.073)	0.744 (0.024)	
	0.3	0.733 (0.056)	0.582 (0.063)	0.648 (0.073)	0.757 (0.035)	0.572 (0.047)	0.699 (0.057)	0.758 (0.023)	0.558 (0.040)	0.736 (0.031)	
	1	0.723 (0.067)	0.717 (0.073)	0.705 (0.063)	0.721 (0.041)	0.716 (0.041)	0.719 (0.046)	0.724 (0.023)	0.720 (0.025)	0.726 (0.023)	
Cox PH	0.1	0.892 (0.047)	0.818 (0.086)	0.830 (0.085)	0.935 (0.026)	0.896 (0.048)	0.904 (0.041)	0.948 (0.013)	0.935 (0.021)	0.940 (0.015)	
	0.3	0.914 (0.042)	0.858 (0.076)	0.869 (0.077)	0.937 (0.025)	0.909 (0.038)	0.917 (0.030)	0.957 (0.011)	0.951 (0.014)	0.951 (0.012)	
	1	0.921 (0.040)	0.937 (0.036)	0.917 (0.045)	0.918 (0.033)	0.947 (0.035)	0.951 (0.024)	0.915 (0.018)	0.959 (0.022)	0.964 (0.011)	
		$(d, r_c) = (100, 0.5)$									
		Estimation									
		$n = 100$		$n = 200$		$n = 500$					
Simulation	gap	C-mix	CURE	Cox PH	C-mix	CURE	Cox PH	C-mix	CURE	Cox PH	
C-mix	0.1	0.773 (0.064)	0.710 (0.087)	0.678 (0.078)	0.798 (0.038)	0.767 (0.057)	0.744 (0.055)	0.804 (0.022)	0.795 (0.024)	0.788 (0.025)	
	0.3	0.781 (0.057)	0.696 (0.103)	0.697 (0.087)	0.798 (0.034)	0.741 (0.064)	0.741 (0.055)	0.800 (0.021)	0.778 (0.036)	0.785 (0.023)	
	1	0.772 (0.064)	0.742 (0.081)	0.760 (0.071)	0.772 (0.044)	0.732 (0.074)	0.771 (0.041)	0.770 (0.028)	0.740 (0.059)	0.771 (0.029)	
CURE	0.1	0.755 (0.070)	0.759 (0.068)	0.692 (0.082)	0.780 (0.044)	0.782 (0.043)	0.752 (0.052)	0.795 (0.025)	0.795 (0.025)	0.785 (0.026)	
	0.3	0.730 (0.077)	0.737 (0.076)	0.674 (0.086)	0.740 (0.042)	0.740 (0.041)	0.708 (0.055)	0.753 (0.028)	0.753 (0.027)	0.740 (0.031)	
	1	0.663 (0.075)	0.660 (0.076)	0.659 (0.064)	0.661 (0.053)	0.661 (0.052)	0.658 (0.050)	0.657 (0.032)	0.657 (0.033)	0.657 (0.034)	
Cox PH	0.1	0.916 (0.069)	0.924 (0.056)	0.837 (0.097)	0.950 (0.028)	0.949 (0.029)	0.911 (0.052)	0.964 (0.012)	0.964 (0.012)	0.951 (0.016)	
	0.3	0.937 (0.047)	0.934 (0.050)	0.863 (0.071)	0.955 (0.026)	0.956 (0.022)	0.925 (0.037)	0.968 (0.012)	0.968 (0.012)	0.958 (0.015)	
	1	0.963 (0.029)	0.967 (0.027)	0.973 (0.024)	0.966 (0.019)	0.970 (0.017)	0.984 (0.012)	0.962 (0.012)	0.966 (0.011)	0.988 (0.006)	

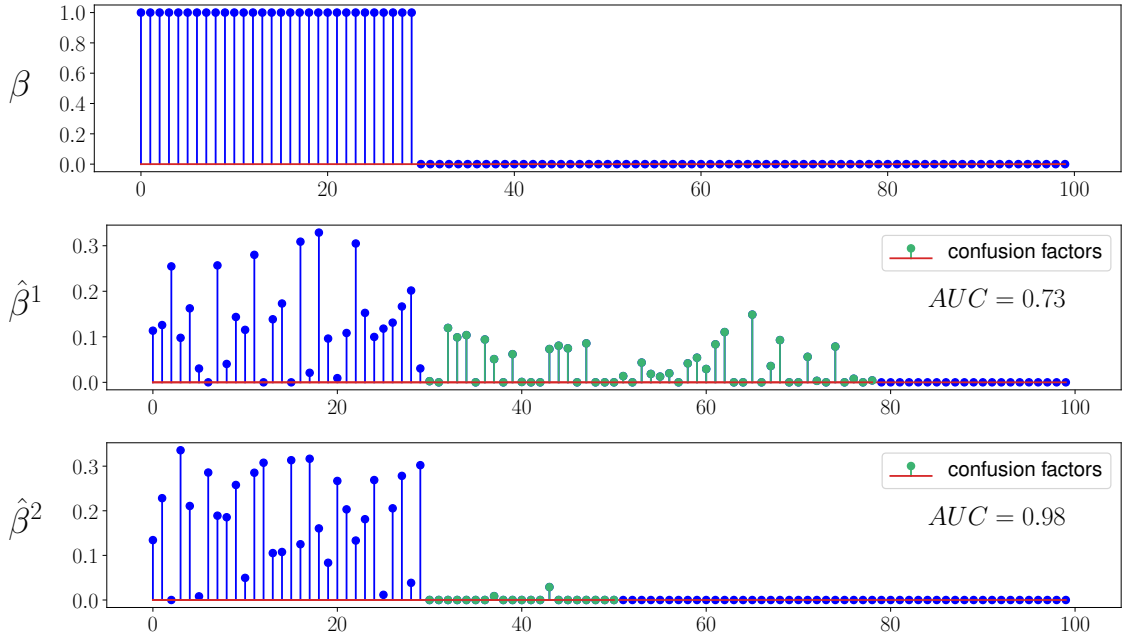


Figure 8: Illustration of the variable selection evaluation procedure. $\hat{\beta}^1$ is learned by the C-mix according to data generated with β and $(\text{gap}, r_{cf}) = (0.2, 0.7)$. We observe that using this gap value to generate data, the model does not succeed to completely vanish the confusion variables (being 70% of the non-active variables, represented in green color), while all other non-active variables are vanished. The corresponding AUC score of feature selection is 0.73. $\hat{\beta}^2$ is learned by the C-mix according to data generated with β and $(\text{gap}, r_{cf}) = (1, 0.3)$. The confusion variables are here almost all detected and the corresponding AUC score of feature selection is 0.98.

G Selected genes per model on the TCGA datasets

In Tables 10, 11 and 12 hereafter, we detail the 20 most significant covariates for each model and for the three considered datasets. For each selected gene, we precise the corresponding effect in percentage, where we define the effect of covariate j as $100 \times |\beta_j| / \|\beta\|_1$ %. Then, to explore physiopathological and epidemiological background that could explain the role of the selected genes in cancer prognosis, we search in MEDLINE (search performed on the 15th september 2016 at <http://www.nlm.nih.gov/bsd/pmresources.html>) the number of publications for different requests: (1) selected gene name (e.g. UBTF), (2) selected gene name and cancer (e.g. UBTF AND cancer[MesH]), (3) selected gene name and cancer survival (e.g. UBTF AND cancer[MesH] AND survival). We then estimate f_1 defined here as the frequency of publication dealing with cancer among all publications for this gene, *i.e.* (2)/(1), and f_2 defined as the frequency of publication dealing with survival among publications dealing with cancer, *i.e.* (3)/(2). A f_1 (respectively f_2) close to 1 just informs that the corresponding gene is well known to be highly related to cancer (respectively to cancer survival) by the genetic research community. Note that the CURE and Cox PH models tend to have a smaller support than the C-mix

one, since they tend to select less than 20 genes.

Table 10: Top 20 selected genes per model for the BRCA cancer, with the corresponding effects. Dots (\cdot) mean zeros.

Genes	Model effects (%)			MEDLINE data		
	C-mix	CURE	Cox PH	(1)	f_1	f_2
PHKB 5257	9.8	7.2	4.3	1079	0.20	0.37
UBTF 7343	7.8	5.8	21.7	14	0.21	\cdot
LOC100132707	5.7	3.9	18.8	\cdot	\cdot	\cdot
CHTF8 54921	4.4	\cdot	7.2	1	1	\cdot
NFKBIA 4792	4.3	1.9	3.4	247	0.27	0.22
EPB41L4B 54566	3.6	2.6	\cdot	19	0.47	0.22
UGP2 7360	3.6	2.2	\cdot	19	0.15	1
DPY19L2P1 554236	3.3	\cdot	3.3	1	\cdot	\cdot
TRMT2B 79979	3.3	2.2	\cdot	\cdot	\cdot	\cdot
HSD3B7 80270	3.2	1.9	7.6	19	0.05	\cdot
DLAT 1737	3.2	2.9	\cdot	75	0.16	0.16
NIPAL2 79815	2.8	1.9	\cdot	\cdot	\cdot	\cdot
FGD3 89846	2.7	\cdot	5.9	10	0.2	0.5
JRKL 8690	2.7	2.6	\cdot	2	\cdot	\cdot
ZBED1 9189	2.5	2.4	\cdot	6	\cdot	\cdot
KCNJ11 3767	2.3	\cdot	\cdot	647	0.02	\cdot
WAC 51322	2.0	3.2	\cdot	260	0.05	0.25
FLT3 2322	2.0	\cdot	\cdot	4435	0.55	0.42
STK3 6788	1.9	2.3	\cdot	107	0.32	0.15
PAOX 196743	1.9	1.9	\cdot	18	0.11	\cdot
C14orf68 283600	\cdot	3.3	\cdot	\cdot	\cdot	\cdot
LIN7C 55327	\cdot	3.1	\cdot	36	0.06	\cdot
PNRC2 55629	\cdot	2.1	\cdot	15	\cdot	\cdot
SLC39A7 7922	\cdot	1.8	\cdot	22	0.18	\cdot
MAGT1 84061	\cdot	1.7	\cdot	50	0.12	0.17
IRF2 3660	\cdot	\cdot	10.9	310	0.21	0.14
PELO 53918	\cdot	\cdot	7.0	265	0.08	0.04
SUSD3 203328	\cdot	\cdot	5.3	5	0.6	0.67
LEF1 51176	\cdot	\cdot	3.2	940	0.29	0.23
CPA4 51200	\cdot	\cdot	1.4	18	0.22	\cdot

Table 11: Top 20 selected genes per model for the GBM cancer, with the corresponding effects. Dots (\cdot) mean zeros.

Genes	Model effects (%)			MEDLINE data		
	C-mix	CURE	Cox PH	(1)	f ₁	f ₂
ARMCX6 54470	4.9	\cdot	23.6	1	\cdot	\cdot
FAM35A 54537	4.4	\cdot	21.8	\cdot	\cdot	\cdot
CLEC4GP1 440508	3.9	5.1	2.8	\cdot	\cdot	\cdot
INSL3 3640	3.6	2.7	1.7	404	0.06	0.12
REM1 28954	3.2	\cdot	\cdot	54	0.05	0.66
FAM35B2 439965	3.0	\cdot	\cdot	\cdot	\cdot	\cdot
TSPAN4 7106	2.7	\cdot	\cdot	16	0.31	0.4
AP3M1 26985	2.7	\cdot	\cdot	2	0.5	\cdot
PXN 5829	2.6	\cdot	15.4	891	0.25	0.18
PDE4C 5143	2.5	\cdot	\cdot	67	0.06	0.25
PGBD5 79605	2.5	\cdot	\cdot	5	0.25	\cdot
NRG1 3084	2.4	\cdot	18.5	1207	0.12	0.29
LOC653786	2.2	\cdot	\cdot	\cdot	\cdot	\cdot
FERMT1 55612	2.1	\cdot	\cdot	115	0.19	0.18
PLD3 23646	2.0	\cdot	\cdot	38	0.10	0.25
MIER1 57708	1.9	\cdot	2.1	16	0.31	\cdot
UTP14C 9724	1.8	\cdot	\cdot	5	0.4	\cdot
AZU1 566	1.8	\cdot	\cdot	15	0.2	0.33
KCNC4 3749	1.7	\cdot	\cdot	30	0.1	0.33
FAM35B 414241	1.6	\cdot	\cdot	\cdot	\cdot	\cdot
CRELD1 78987	\cdot	32.2	\cdot	32	0.03	\cdot
HMG5 79366	\cdot	21.2	\cdot	41	0.54	0.32
PNLDC1 154197	\cdot	12.2	\cdot	3	\cdot	\cdot
LOC493754	\cdot	9.8	\cdot	\cdot	\cdot	\cdot
KIAA0146 23514	\cdot	8.7	\cdot	3	0.67	\cdot
TMCO655374	\cdot	3.6	\cdot	4	0.25	\cdot
ABLIM1 3983	\cdot	2.1	\cdot	20	0.2	\cdot
OSBPL11 114885	\cdot	1.0	\cdot	\cdot	\cdot	\cdot
TRAPPC1 58485	\cdot	0.9	\cdot	4	0.75	\cdot
TBCEL 219899	\cdot	0.5	\cdot	7	0.28	\cdot
RPL39L 116832	\cdot	\cdot	8.8	10	0.7	0.14
GALE 2582	\cdot	\cdot	3.5	540	0.02	\cdot
BBC3 27113	\cdot	\cdot	0.7	561	0.54	0.38
DUSP6 1848	\cdot	\cdot	0.6	307	0.30	0.22

Table 12: Top 20 selected genes per model for the KIRC cancer, with the corresponding effects. Dots (·) mean zeros.

Genes	Model effects (%)			MEDLINE data		
	C-mix	CURE	Cox PH	(1)	f ₁	f ₂
BCL2L12 83596	8.6	2.7	·	64	0.72	0.39
MARS 4141	7.5	6.9	7.2	577	0.02	0.1
NUMBL 9253	7.2	28.6	3.3	56	0.14	0.25
CKAP4 10970	6.1	10.6	22.3	825	0.63	0.11
HN1 51155	5.8	3.8	·	13	0.38	0.2
GIPC2 54810	5.7	·	·	15	0.6	0.11
NPR3 4883	5.2	·	·	105	0.05	0.6
GBA3 57733	5.0	·	·	19	0.10	·
SLC47A1 55244	5.0	·	·	70	0.06	·
ALDH3A2 224	4.7	·	2.6	52	0.06	0.33
CCNF 899	4.2	2.8	·	50	0.24	0.08
EHHADH 1962	3.9	·	·	90	0.1	·
SGCB 6443	3.3	·	·	30	·	·
GFPT2 9945	2.7	1.3	·	18	0.22	0.25
PPAP2B 8613	2.3	·	·	29	0.17	0.2
MBOAT7 79143	1.9	13.8	11.1	15	·	·
OSBPL1A 114876	1.5	·	·	7	·	·
C16orf57 79650	1.2	·	·	26	·	·
ATXN7L3 56970	0.9	2.5	·	9	·	·
C16orf59 80178	0.8	·	·	3	0.66	·
STRADA92335	·	20.7	53.5	9	·	·
ABCC10 89845	·	3.9	·	80	0.32	0.23
MDK 4192	·	1.2	·	789	0.38	0.23
C16orf59 80178	·	1.1	·	3	0.6	·

References

- Ash A Alizadeh, Michael B Eisen, R Eric Davis, Chi Ma, Izidore S Lossos, Andreas Rosenwald, Jennifer C Boldrick, Hajeer Sabet, Truc Tran, Xin Yu, et al. Distinct types of diffuse large b-cell lymphoma identified by gene expression profiling. *Nature*, 403(6769):503–511, 2000.
- Galen Andrew and Jianfeng Gao. Scalable training of l1-regularized log-linear models. In *International Conference on Machine Learning*, pages 33–40. ACM, 2007.
- Jeffrey D Banfield and Adrian E Raftery. Model-based gaussian and non-gaussian clustering. *Biometrics*, pages 803–821, 1993.
- David G Beer, Sharon LR Kardia, Chiang-Ching Huang, Thomas J Giordano, Albert M Levin, David E Misek, Lin Lin, Guoan Chen, Tarek G Gharib, Dafydd G Thomas, et al. Gene-expression profiles predict survival of patients with lung adenocarcinoma. *Nature medicine*, 8(8):816–824, 2002.
- D. P. Bertsekas. *Nonlinear programming*. Athena Scientific, Belmont, MA, 1995.
- Arindam Bhattacharjee, William G Richards, Jane Staunton, Cheng Li, Stefano Monti, Priya Vasa, Christine Ladd, Javad Beheshti, Raphael Bueno, Michael Gillette, et al. Classification of human lung carcinomas by mrna expression profiling reveals distinct adenocarcinoma subclasses. *Proceedings of the National Academy of Sciences*, 98(24):13790–13795, 2001.
- Paul Blanche, Aurélien Latouche, and Vivian Viallon. Time-dependent auc with right-censored data: A survey. *Risk Assessment and Evaluation of Predictions*, 215:239–251, 2013.
- Stephen Boyd and Lieven Vandenberghe. *Convex optimization*. Cambridge university press, 2004.
- Norman E Breslow. Contribution to the discussion of the paper by dr cox. *Journal of the Royal Statistical Society, Series B*, 34(2):216–217, 1972.
- D. R. Cox. Regression models and life-tables. *Journal of the Royal Statistical Society, Series B (Methodological)*, 34(2):187–220, 1972.
- R De Angelis, R Capocaccia, T Hakulinen, B Soderman, and A Verdecchia. Mixture models for cancer survival analysis: application to population-based data with covariates. *Statistics in medicine*, 18(4):441–454, 1999.
- AP Dempster, NM Laird, and DB Rubin. Maximum likelihood from incomplete data via the em algorithm. *Journal of the Royal Statistical Society, Series B (Methodological)*, 39(1):1–38, 1977.
- Jianqing Fan, Yang Feng, Yichao Wu, et al. High-dimensional variable selection for coxs proportional hazards model. In *Borrowing Strength: Theory Powering Applications—A Festschrift for Lawrence D. Brown*, pages 70–86. Institute of Mathematical Statistics, 2010.

- VT Farewell. The use of mixture models for the analysis of survival data with long-term survivors. *Biometrics*, 38(4):1041–1046, 1982.
- Todd R Golub, Donna K Slonim, Pablo Tamayo, Christine Huard, Michelle Gaasenbeek, Jill P Mesirov, Hilary Coller, Mignon L Loh, James R Downing, Mark A Caligiuri, et al. Molecular classification of cancer: class discovery and class prediction by gene expression monitoring. *science*, 286(5439):531–537, 1999.
- Frank E Harrell, Kerry L Lee, and Daniel B Mark. Tutorial in biostatistics multivariable prognostic models: issues in developing models, evaluating assumptions and adequacy, and measuring and reducing errors. *Statistics in medicine*, 15: 361–387, 1996.
- Trevor Hastie, Robert Tibshirani, David Botstein, and Patrick Brown. Supervised harvesting of expression trees. *Genome Biology*, 2(1):research0003–1, 2001.
- Patrick J Heagerty and Yingye Zheng. Survival model predictive accuracy and roc curves. *Biometrics*, 61(1):92–105, 2005.
- Patrick J Heagerty, Thomas Lumley, and Margaret S Pepe. Time-dependent roc curves for censored survival data and a diagnostic marker. *Biometrics*, 56(2): 337–344, 2000.
- Edward L Kaplan and Paul Meier. Nonparametric estimation from incomplete observations. *Journal of the American statistical association*, 53(282):457–481, 1958.
- Md Hasinur Rahaman Khan and J Ewart H Shaw. Variable selection for survival data with a class of adaptive elastic net techniques. *Statistics and Computing*, 26(3):725–741, 2016.
- John P Klein and Melvin L Moeschberger. *Survival analysis: techniques for censored and truncated data*. Springer Science & Business Media, 2005.
- Anthony YC Kuk and Chen-Hsin Chen. A mixture model combining logistic regression with proportional hazards regression. *Biometrika*, 79(3):531–541, 1992.
- Lynn Kuo and Fengchun Peng. A mixture-model approach to the analysis of survival data. *Biostatistics-Basel-*, 5:255–272, 2000.
- B. N. Mukherjee and S. S. Maiti. On some properties of positive definite toeplitz matrices and their possible applications. *Linear algebra and its applications*, 102: 211–240, 1988.
- Thordur Oskarsson, Swarnali Acharyya, Xiang HF Zhang, Sakari Vanharanta, So-hail F Tavazoie, Patrick G Morris, Robert J Downey, Katia Manova-Todorova, Edi Brogi, and Joan Massagué. Breast cancer cells produce tenascin c as a metastatic niche component to colonize the lungs. *Nature medicine*, 17(7):867–874, 2011.
- Andreas Rosenwald, George Wright, Wing C Chan, Joseph M Connors, Elias Campo, Richard I Fisher, Randy D Gascoyne, H Konrad Muller-Hermelink, Erlend B Smeland, Jena M Giltneane, et al. The use of molecular profiling to predict

- survival after chemotherapy for diffuse large-b-cell lymphoma. *New England Journal of Medicine*, 346(25):1937–1947, 2002.
- Diego Franco Saldana and Yang Feng. Sis: An r package for sure independence screening in ultrahigh dimensional statistical models. *Journal of Statistical Software*, 2016.
- Margaret A Shipp, Ken N Ross, Pablo Tamayo, Andrew P Weng, Jeffery L Kutok, Ricardo CT Aguiar, Michelle Gaasenbeek, Michael Angelo, Michael Reich, Geraldine S Pinkus, et al. Diffuse large b-cell lymphoma outcome prediction by gene-expression profiling and supervised machine learning. *Nature medicine*, 8(1): 68–74, 2002.
- Noah Simon, Jerome Friedman, Trevor Hastie, Rob Tibshirani, et al. Regularization paths for coxs proportional hazards model via coordinate descent. *Journal of statistical software*, 39(5):1–13, 2011.
- Therese Sørlie, Charles M Perou, Robert Tibshirani, Turid Aas, Stephanie Geisler, Hilde Johnsen, Trevor Hastie, Michael B Eisen, Matt Van De Rijn, Stefanie S Jeffrey, et al. Gene expression patterns of breast carcinomas distinguish tumor subclasses with clinical implications. *Proceedings of the National Academy of Sciences*, 98(19):10869–10874, 2001.
- Robert Tibshirani, Trevor Hastie, Balasubramanian Narasimhan, and Gilbert Chu. Diagnosis of multiple cancer types by shrunken centroids of gene expression. *Proceedings of the National Academy of Sciences*, 99(10):6567–6572, 2002.
- Paul Tseng. Convergence of a block coordinate descent method for nondifferentiable minimization. *Journal of optimization theory and applications*, 109(3):475–494, 2001.
- Hajime Uno, Tianxi Cai, Michael J Pencina, Ralph B D’Agostino, and LJ Wei. On the c-statistics for evaluating overall adequacy of risk prediction procedures with censored survival data. *Statistics in medicine*, 30(10):1105–1117, 2011.
- Laura J Van’t Veer, Hongyue Dai, Marc J Van De Vijver, Yudong D He, Augustinus AM Hart, Mao Mao, Hans L Peterse, Karin van der Kooy, Matthew J Marton, Anke T Witteveen, et al. Gene expression profiling predicts clinical outcome of breast cancer. *nature*, 415(6871):530–536, 2002.
- Lee-Jen Wei. The accelerated failure time model: a useful alternative to the cox regression model in survival analysis. *Statistics in medicine*, 11(14-15):1871–1879, 1992.
- CF Jeff Wu. On the convergence properties of the em algorithm. *The Annals of Statistics*, 11:95–103, 1983.
- Yamei Zhou, Christina Yau, Joe W Gray, Karen Chew, Shanaz H Dairkee, Dan H Moore, Urs Eppenberger, Serenella Eppenberger-Castori, and Christopher C Benz. Enhanced $\text{nf}\kappa\text{b}$ and ap-1 transcriptional activity associated with antiestrogen resistant breast cancer. *BMC cancer*, 7(1):1, 2007.

Ciyou Zhu, Richard H Byrd, Peihuang Lu, and Jorge Nocedal. Algorithm 778: L-bfgs-b: Fortran subroutines for large-scale bound-constrained optimization. *ACM Transactions on Mathematical Software (TOMS)*, 23(4):550–560, 1997.

Hui Zou and Trevor Hastie. Regularization and variable selection via the elastic net. *Journal of the Royal Statistical Society: Series B (Statistical Methodology)*, 67(2): 301–320, 2005.